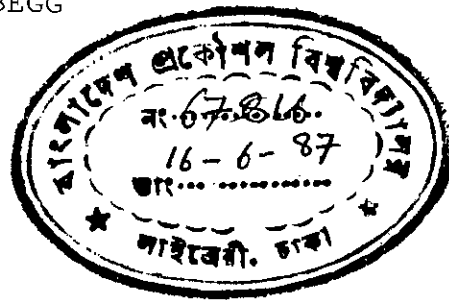


CALCULATION OF ELECTROMECHANICAL STRESS DISTRIBUTION  
IN INSULATORS USING FINITE ELEMENT METHOD

BY  
MD. REZAUL KARIM BEGG



A THESIS  
SUBMITTED TO THE DEPARTMENT OF ELECTRICAL AND ELECTRONIC  
ENGINEERING IN PARTIAL FULFILMENT OF THE REQUIREMENTS FOR  
THE DEGREE  
OF  
MASTER OF SCIENCE IN ENGINEERING (ELECTRICAL AND ELECTRONIC)



#67816#

DEPARTMENT OF ELECTRICAL AND ELECTRONIC ENGINEERING,  
BANGLADESH UNIVERSITY OF ENGINEERING AND TECHNOLOGY, DHAKA.  
MAY 1987.

CERTIFICATE

This is to certify that this work has been done by me and it has not been submitted elsewhere for the award of any degree or diploma.

Signature of the student

*9mbeg 13/5/87*  
( Md. Rezaul Karim Begg. )

Accepted as satisfactory for partial fulfilment of the requirements for the degree of M.Sc. Engineering in Electrical and Electronic Engineering.

BOARD OF EXAMINERS

- i) M. A. Matin 19.5.1987  
 (Dr. Md. Abdul Matin)  
 Associate Professor  
 Dept. of Electrical and  
 Electronic Engg. BUET, Dhaka. Chairman  
 and  
 Supervisor
- ii) শামসুদ্দিন আহমেদ ১৯.৫.৮৭  
 (Prof. Dr. Shamsuddin Ahmed)  
 Chief Instructor,  
 Dept. of Electrical and  
 Electronic Engineering  
 Islamic Centre for Technical and  
 Vocational Training and Research  
 Tongi, Dhaka. Co-supervisor
- iii) শহীদ মুজিবুর রহমান ১৯.৫.৮৭  
 (Prof. Dr. Md. Mujibur Rahman)  
 Professor and Head  
 Dept. of Electrical and Electronic  
 Engineering, BUET, Dhaka. Member
- iv) Saiful Islam  
 (Dr. Saiful Islam.)  
 Associate Professor  
 Dept. of Electrical and Electronic  
 Engineering, BUET, Dhaka. Member
- v) নাজরুল ইসলাম  
 ( Dr. Nazrul Islam )  
 Chairman, Bangladesh Tea Board,  
 Ex-Member, Planning Commission  
 Ex-Chairman, Bangladesh Steel and Engg.  
 Corporation, Road No.17, House No.61  
 Block-E, Banani, Dhaka. Member-External

### ACKNOWLEDGEMENT

Praise be to Allah, Lord of the Worlds, the Almighty, with whose gracious help it was possible to accomplish this task.

The author would express his deep sense of gratitude to Prof. Shamsuddin Ahmed, former Dean of the Faculty of Electrical and Electronic Engineering, BUET, Dhaka, who supervised the work at its initial stage and was a constant source of encouragement and guidance till the completion of the thesis. The author wishes to express his heart-felt gratitude and sincere thanks to his adviser, Dr. Md. Abdul Matin, Associate Professor of the Department of Electrical and Electronic Engineering, BUET, for his kind guidance, constant encouragement and supervision throughout the course of this research.

The author would like to acknowledge with thanks the advice and inspiration from Dr. Md. Mujibur Rahman, Prof. and Head, Department of Electrical and Electronic Engineering, BUET, Dhaka.

The author would acknowledge sincere thanks to Dr. S.F. Rahman, Prof. and Dean, Faculty of Electrical and Electronic Engineering, for his valuable suggestion and deep interest into the project and to Dr. Saiful Islam,

Associate Prof., Department of Electrical and Electronic Engineering, BUET, Dhaka for valuable suggestions and encouragement.

The author would express his deep sense of gratitude to Dr. Nazrul Islam, Chairman Bangladesh Tea Board, Ex-Chairman Bangladesh Steel and Engineering Corporation and an Ex-member of Bangladesh Planning Commission for kindly illuminating the discussions by his presence in the Board of oral examination.

The author would express his sincere gratitude to Prof. J.R. Chowdhury, the Director, Computer Centre, BUET for his kind permission for working at a computer terminal where almost all the computations were made. The author would thankfully appreciate the co-operation of all staff of the BUET Computer Centre.

Finally the author would express thanks to all staff of the Faculty of Electrical and Electronic Engineering for help and assistance.

ABSTRACT

Electromechanical stress distribution in a dielectric between two circular parallel plates has been calculated using finite element method. First, the space between two circular parallel plates has been divided into a finite number of triangular elements. An extremum function in energy density form has been developed. Then using energy minimization technique, the potential at different vertices of the elements are calculated. A computer program has been developed for calculating fields, electromechanical stresses developed in both isotropic and anisotropic dielectrics between parallel circular plates. Later on, the same method has been extended to find electromechanical stress distributions for a non-linear medium like ferroelectric insulator. Effects of both electrostatic and alternating fields on the electromechanical stress distributions in ferroelectric materials have been studied.

CONTENTS

	<u>Page</u>
CHAPTER 1 GENERAL INTRODUCTION	
1.1 Historical review	1
1.2 Present state of art of the Project	2
1.3 Objective of the research	3
1.4 Procedure and methodology	3
CHAPTER 2 FINITE ELEMENT FORMULATION OF THE PROBLEM IN A DIELECTRIC	
2.1 Laplace's equation	5
2.2 Solution by finite element method using triangular elements in an isotropic dielectric.	6
2.3 Finite element solution in anisotropic dielectric	13
2.4 Potential distribution in an isotropic dielectric between two parallel circular plates.	16
2.5 Potential distribution in an anisotropic dielectric between two parallel circular plates.	18
2.6 Discussion	21
CHAPTER 3 ELECTROMECHANICAL STRESS DISTRIBUTION IN INSULATORS	
3.1 Introduction	23
3.2 Electromechanical stress analysis for a dielectric medium.	

## Contents contd.

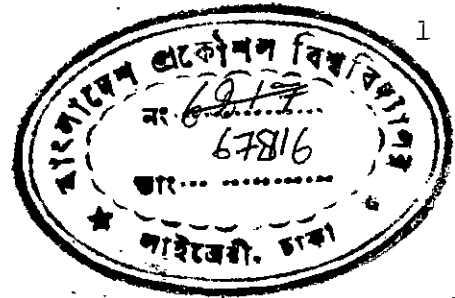
	<u>Page</u>
3.3 Electromechanical stress distribution in an isotropic dielectric between two parallel circular plates.	35
3.4 Electromechanical stress distribution in an anisotropic dielectric between two parallel circular plates.	46
3.5 Discussion	54
CHAPTER 4 ELECTROMECHANICAL STRESS DISTRIBUTION IN FERROELECTRIC INSULATORS.	
4.1 Introduction	56
4.2 Review of the properties of ferroelectric materials.	57
4.3 Electromechanical stress analysis in a ferroelectric medium.	61
4.4 Electromechanical stress distribution in a ferroelectric insulator between two circular parallel plates.	65
4.5 Discussion	79
CHAPTER 5 GENERAL DISCUSSION AND CONCLUSION	81
Appendix	85
Computer Program	90
References.	102



LIST OF PRINCIPAL SYMBOLS

$\bar{E}$	Electric stress or field vector (v/m)
$\bar{D}$	Electric flux density, coulomb/m <sup>2</sup>
$\rho$	Charge density , coulomb/m <sup>3</sup>
$\epsilon_r$	Relative permittivity
$\epsilon_0$	Permittivity of free space, farad/m
$\phi$	Potential (Volts)
J	Extremum function
$S^e$	Element submatrix
$\hat{\epsilon}_r$	Permittivity tensor of anisotropic dielectric
a	Radius of upper circular plate, cm
b	Radius of lower circular plate, cm
h	Distance between the two circular parallel plates, cm
$\hat{S}$	Electromechanical stress tensor
$S_{ij}$	Components of the tensor $\hat{S}$
$\bar{i}$	Unit column vector
$\bar{F}$	Electro-mechanical force, Newton
$\bar{n}$	Unit outward normal to a surface or contour
$\bar{p}$	Polarization in coulomb./m <sup>2</sup>
$\bar{t}$	Electro-mechanical stress vector
$P_r$	Remanant polarization in coulomb./m <sup>2</sup>
$\epsilon_{ro}$	Dielectric constant at very weak field
$E_s$	Saturation electric field of ferroelectric material, volt/m.

CHAPTER 1  
GENERAL INTRODUCTION



1.1 HISTORICAL REVIEW

Electrical insulation technology has been developed gradually and empirically from the beginning of Electrical Engineering. It is required from the stand-point of safety and protection from high voltages and the reduction of power loss and economic operation of power and communication networks. This will cause the proportional increase in the size of system apparatus. Improvement and compactness of design of system apparatus would have a far-reaching influence on the cost reduction and savings of energy resources. So, electrical insulators should be designed to withstand the higher electro-mechanical stress in order to develop compact and high voltage equipments.

In high voltage insulators space charge can lead to very undesirable consequences. Various effects of space charge in insulators have been summarized by Ieda[1],[2]. He showed that the developed space charge alters the distribution profile of the field in comparison with the original field. It is known that the formation of space charge depends whether the field is uniform or non-uniform.

Flash-over takes place along the insulator surface if the tangential field is high enough to sustain a discharge.

Singer and Weiss [3] optimized high voltage insulator shape making tangential field distributions uniform along its surface. Another method to optimize the field stress on HV insulators has been described by Salam [4].

Physical systems are so complex that the analytical solution of Laplace's or Poisson's equation is difficult. As such with the increasing availability of high speed digital computers, various numerical techniques are being extensively developed for the calculation of electrostatic fields in high voltage systems. Mukherjee and Roy [5] calculated fields in insulators using fictitious point charge method and he was successful in applying this method for disc insulators. Takeshi [6] used charge simulation method in combination with the method of images to find electric fields in dielectric multi-layers. Tadasu [7] successfully applied charge simulation method to study the field behaviour at points on the boundary of two dielectrics. Heng Kun [8] suggests that the field distribution along the insulator surface is strongly dependent on the  $\rho$ -E characteristics and the extension of the semiconductor coating as well as the frequency of the operating voltages.

## 1.2 PRESENT STATE OF ART OF THE PROJECT

Finite element numerical technique is now being extensively used to find solution of Laplace's equation encountered in

problems related to civil, mechanical and electrical engineering. Chang et al. [9] used finite element method to calculate electrical stress distribution within dielectric cavities. Ahmed [10] used this method to solve waveguide problems. Monopolar corona equation was solved by Salam [11] using modified finite element method. The finite element method is a powerful numerical technique that can be precisely used to solve boundary value problems by piecewise linearization of the potential function over a large number of discrete spatial elements. It received considerable research interest in designing civil and mechanical engineering structures.

### 1.3 OBJECTIVE OF THE RESEARCH

The objective of this research is to calculate the electromechanical stress distribution in insulators by finite element method. The purpose of this analysis is to predict the points of concentrated stresses and the air-flash-over voltages of insulators. It is also of interest to see the electrostrictive effects on the electrostatic stresses developed in ferroelectric insulators.

### 1.4 PROCEDURE AND METHODOLOGY

In electromechanical stress calculation, the insulator region will be first divided into a finite number of polygonal

sub-regions called elements. Then using finite element method the potential distributions as well as electric stress at different vertices will be calculated. A suitable energy distribution function in variational form will be developed for the systems under consideration and from the energy distribution function the desired stress will be obtained. Computer programmes will be developed to handle boundary value problems with some open boundaries by using finite element variational technique.

Chapter-2 describes in general manner the finite element formulation of Laplace's equation in isotropic and anisotropic dielectrics. Potential distribution in a dielectric between two parallel circular plates is also illustrated for isotropic and anisotropic cases. Electromechanical stress distribution in dielectric regions between two parallel circular plates are derived in chapter-3. Chapter-4 discusses the electrostrictive effects on the stress distribution in ferroelectric insulators. The thesis is concluded with a general discussion in chapter-5.

## CHAPTER 2

## FINITE ELEMENT FORMULATION OF THE PROBLEM IN A DIELECTRIC

2.1 LAPLACE'S EQUATION:

The equations satisfied by the field of a stationary charge distribution follow directly from Maxwell's equations when all the time derivatives are placed to zero. We have, then, at all regular points of an electrostatic field  $\bar{E}$

$$\nabla \times \bar{E} = 0 \quad \dots \quad (2.1)$$

$$\nabla \cdot \bar{D} = \rho \quad \dots \quad (2.2)$$

Where  $\bar{D}$  is the electric flux density and  $\rho$  is the charge density. According to (2.1), the line integral of the field intensity  $\bar{E}$  around any closed path is zero and the field is conservative. The conservative nature of the field is a necessary and sufficient condition for the existence of a scalar potential  $\phi$  whose negative gradient gives the electrostatic field,

$$\bar{E} = - \nabla \phi \quad \dots \quad (2.3)$$

For linear isotropic medium we can write

$$\bar{D} = \epsilon \bar{E} = - \epsilon \nabla \phi$$

where  $\epsilon$  is the permittivity of the medium.

From (2.2)

$$\nabla \cdot (-\epsilon \nabla \phi) = -\epsilon \nabla^2 \phi + \nabla \epsilon \cdot \nabla \phi = \rho$$

Since  $\nabla \epsilon = 0$  for isotropic homogeneous dielectric,

$$\nabla^2 \phi = -\frac{\rho}{\epsilon} \quad \dots \quad (2.4)$$

This is Poisson's equation. At points of the field which are charge free (2.4) reduces to Laplace's equation,

$$\nabla^2 \phi = 0 \quad \dots \quad (2.5)$$

## 2.2 SOLUTION BY FINITE ELEMENT METHOD USING TRIANGULAR ELEMENTS IN AN ISOTROPIC DIELECTRIC.

The basic requirement of the development of finite element equations is to find an extremum function which can be written in energy density form. As a first step in the development of this method, a uniform surface is considered which is completely filled with homogeneous and isotropic dielectric.

✓ The extremum function for electrostatic field can be written as

$$J(\phi) = \frac{1}{2} \iint |\nabla \phi|^2 ds \quad \dots \quad (2.6)$$

Derivation of eqn. (2.6) is given in Appendix -A1.

The finite element method [12]-[13] employs a set of algebraic functions defined over a subsection of the whole cross-section. These subsections may be polygonal in shape and are called elements. Thus in the finite element method

the entire domain over which the operator is defined is divided into a finite number of elements on each of which the actual mode function is approximated by a set of continuous algebraic functions which are only defined over the particular element under consideration and are linearly dependent on the values of  $\phi$  at the vertices of the element.

Hence, if an element has  $n$  vertices (for triangular element  $n=3$ ), the potential  $\phi$  within it may be approximated by

$$\phi(x,y) = \sum_{k=1}^n N_k(x,y) \phi_k \dots (2.7)$$

Where  $\phi_k$  is the value of  $\phi$  at the vertex  $k$  and  $N_k(x,y)$  is a predetermined algebraic function which is uniquely defined and differentiable over the element and which reduces to zero outside the element.

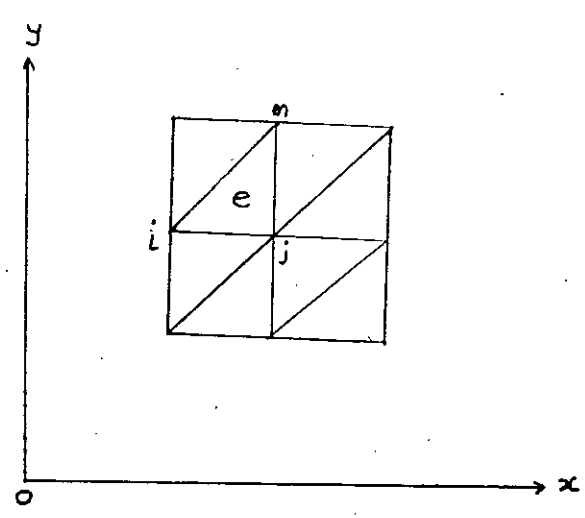


Fig. 1: Division into triangular elements.



An arbitrary isotropic dielectric cross section with the scheme of grading into elements is shown in Fig. 1. Triangular elements are considered here. A typical element (the  $e$ th element) is described by the vertices  $i, j$  and  $m$  in cyclic order. Let  $\phi_i, \phi_j$  and  $\phi_m$  be the corresponding values of  $\phi$  at the vertices. For the element  $e$  the functional dependence of  $\phi(x, y)$  can be written as

$$\phi^e(x, y) = \alpha_0 + \alpha_1 x + \alpha_2 y \quad \dots \quad (2.8)$$

where  $\alpha_0, \alpha_1$  and  $\alpha_2$  are to be determined.

If  $(x_i, y_i), (x_j, y_j)$  and  $(x_m, y_m)$  are the co-ordinates of the vertices  $i, j$  and  $m$ , then solving for  $\alpha_0, \alpha_1$  and  $\alpha_2$ , we obtain

$$\phi^e(x, y) = \frac{1}{2A} \left[ (a_i + b_i x + c_i y) \phi_i^e + (a_j + b_j x + c_j y) \phi_j^e + (a_m + b_m x + c_m y) \phi_m^e \right] \quad \dots \quad (2.9)$$

where

$$a_i = x_j y_m - x_m y_j \quad \dots \quad (2.10)$$

$$b_i = y_j - y_m$$

$$c_i = x_m - x_j$$

$A$  = area of the triangular element.

$$\text{and } A = \frac{1}{2} \begin{vmatrix} 1 & x_i & y_i \\ 1 & x_j & y_j \\ 1 & x_m & y_m \end{vmatrix}$$

The values of the other parameters can be obtained by a cyclic rotation of the suffices  $i, j, m$ .

It is important to note that the functional form of the potential  $\phi^e(x, y)$  as described by eqn. (2.9) for all the elements of the entire domain satisfies the continuity relation throughout the whole region. This continuity of  $\phi$  is essential for the validity of the variational expression. The finite jump in the normal derivative will not introduce any error in the variational formulation, because the contribution of this type of discontinuity in the normal derivative to the net integrated value of the function  $J$  is always zero.

When the functional form of  $\phi$  as given above is substituted into eqn. (2.6) and the corresponding integrations are carried out,  $J$  will be a function of the variables  $\phi_k$ . If there are  $M$  vertices, then

$$J(\phi) = F(\phi_1, \phi_2, \phi_3, \dots, \phi_M) \quad \dots \quad (2.11)$$

The optimum value of a set of  $\phi_k$  for a certain functional form of  $N_k(x,y)$  may be obtained by minimizing the function given by eqn. (2.11) with respect to each of  $\phi_k$  i.e., equating  $\frac{\partial J}{\partial \phi_k} = 0$  ; for  $k = 1, 2, 3 \dots \dots M$  (2.12)

However, in the vicinity of boundaries where constant potentials are specified

$$J \rightarrow \frac{1}{2} \phi^2$$

So that at the boundary,  $\frac{\partial J}{\partial \phi} \rightarrow \phi_b$

where  $\phi_b$  is the value of the potential at the boundary.

Eqn. (2.6) can be written for a two-dimensional case

$$\begin{aligned} J &= \frac{1}{2} \iint |\nabla \phi|^2 ds \\ &= \frac{1}{2} \iint \left[ \left( \frac{\partial \phi}{\partial x} \right)^2 + \left( \frac{\partial \phi}{\partial y} \right)^2 \right] dx dy \end{aligned}$$

For the eth element.

$$J^e = \frac{1}{2} \iint_e \left[ \left( \frac{\partial \phi^e}{\partial x} \right)^2 + \left( \frac{\partial \phi^e}{\partial y} \right)^2 \right] dx dy \dots \quad (2.13)$$

From eqn. (2.9) taking partial derivative with respect to  $x$  and  $y$

$$\frac{\partial \phi^e}{\partial x} = \frac{1}{2A} x (b_i \phi_i + b_j \phi_j + b_m \phi_m) \dots \quad (2.14)$$

$$\text{and } \frac{\partial \phi^e}{\partial y} = \frac{1}{2A} \times (c_i \phi_i + c_j \phi_j + c_m \phi_m) \quad \dots \quad (2.15)$$

Putting the eqns. (2.14) and (2.15) into eqn. (2.13) we get

$$J^e = \frac{1}{8A^2} \iint_{e_i} \left[ (b_i \phi_i + b_j \phi_j + b_m \phi_m)^2 + (c_i \phi_i + c_j \phi_j + c_m \phi_m)^2 \right] dx dy \quad \dots \quad (2.16)$$

The integrand is independent of x & y

So, using  $\iint_{e_i} dx dy = A$

$$J^e = \frac{1}{8A} \left[ (b_i \phi_i + b_j \phi_j + b_m \phi_m)^2 + (c_i \phi_i + c_j \phi_j + c_m \phi_m)^2 \right] \dots \quad (2.17)$$

Using eqn. (2.12) for the minimization of J functional over the element e

$$\frac{\partial J^e}{\partial \phi_i} = \frac{1}{4A} \left[ b_i (b_i \phi_i + b_j \phi_j + b_m \phi_m) + c_i (c_i \phi_i + c_j \phi_j + c_m \phi_m) \right]$$

$$\frac{\partial J^e}{\partial \phi_j} = \frac{1}{4A} \left[ b_j (b_i \phi_i + b_j \phi_j + b_m \phi_m) + c_j (c_i \phi_i + c_j \phi_j + c_m \phi_m) \right]$$

$$\frac{\partial J^e}{\partial \phi_m} = \frac{1}{4A} \left[ b_m (b_i \phi_i + b_j \phi_j + b_m \phi_m) + c_m (c_i \phi_i + c_j \phi_j + c_m \phi_m) \right] \dots \quad (2.18)$$

In matrix form for the element e with nodes i, J, m

$$\begin{bmatrix} \frac{\partial J^e}{\partial \phi_i} \\ \frac{\partial J^e}{\partial \phi_j} \\ \frac{\partial J^e}{\partial \phi_m} \end{bmatrix} = \begin{bmatrix} b_i^2 + c_i^2 & b_i b_j + c_i c_j & b_i b_m + c_i c_m \\ b_i b_j + c_i c_j & b_j^2 + c_j^2 & b_j b_m + c_j c_m \\ b_i b_m + c_i c_m & b_j b_m + c_j c_m & b_m^2 + c_m^2 \end{bmatrix} \begin{bmatrix} \phi_i \\ \phi_j \\ \phi_m \end{bmatrix} \dots \quad (2.19)$$

$$\text{or} \quad \begin{bmatrix} \frac{\partial J^e}{\partial \phi^e} \end{bmatrix} = [s^e] \cdot [\phi^e] \dots \quad (2.20)$$

where

$S^e$  is the element sub-matrix and  $\phi^e$  is a column matrix.  $S^e$  is a square symmetric matrix such that  $S_{ij}^e = S_{ji}^e$ . For triangular elements, each of the element sub-matrix is a 3 x 3 square symmetric matrix. The above equations (2.18) and hence (2.19) can be applied to obtain element sub-matrices for all the elements of the domain. The resultant matrix will be the sum of all the element sub-matrices generated by all the elements.

### 2.3 FINITE ELEMENT SOLUTION IN ANISOTROPIC DIELECTRIC BETWEEN TWO PARALLEL CIRCULAR PLATES

Anisotropic property in materials develops due to nonuniform rate of deformation in different directions. Systems undergoing plastic deformation are in this category. In the case of insulators between two electrodes the rate of deformation due to electro-mechanical stress in the axial direction is expected to be different from that in the lateral directions.

In isotropic dielectrics, polarization is parallel [18] with the applied fields and is independent of the direction of fields. For anisotropic dielectric this is different. An electric field applied to an anisotropic material along an axis of an arbitrarily oriented co-ordinate system leads to polarization which has components in all co-ordinate directions. Hence, Laplace's equation will be modified. The electric flux density is given by

$$\bar{D} = \epsilon_0 \hat{\epsilon}_r \bar{E}$$

where  $\hat{\epsilon}_r$  is the relative permittivity tensor.

$$\text{Now } E = -\nabla\phi \quad (2.21)$$

$$\text{Since } \nabla \cdot D = \rho \quad (2.22)$$

$$\text{Then } \nabla \cdot \epsilon_0 \hat{\epsilon}_r \bar{E} = \rho \quad (2.23)$$

Let us first consider a medium characterized by the uniaxially anisotropic dielectric tensor of dimension  $3 \times 3$ .

$$\hat{\epsilon}_r = \begin{bmatrix} 1 & 0 & 0 \\ 0 & 1 & 0 \\ 0 & 0 & k' \end{bmatrix} \dots \quad (2.24)$$

Now,  $\nabla \cdot \epsilon_0 \hat{\epsilon}_r \nabla \phi = -\rho$

or  $\nabla \cdot \hat{\epsilon}_r \nabla \phi = -\frac{\rho}{\epsilon_0} \dots \quad (2.25)$

This is Poisson's equation for anisotropic medium and the corresponding Laplace's equation is:

$$\nabla \cdot \hat{\epsilon}_r \nabla \phi = 0 \dots \quad (2.26)$$

This takes the form

$$\nabla \cdot \hat{\epsilon}_r \nabla \phi = \frac{\partial^2 \phi}{\partial x^2} + \frac{\partial^2 \phi}{\partial y^2} + k' \frac{\partial^2 \phi}{\partial z^2} = 0 \dots \quad (2.27)$$

This equation is valid also for a biaxial dielectric having dielectric tensor of the form

$$\hat{\epsilon}_r = \begin{bmatrix} 1 & +jk'' & 0 \\ -jk'' & 1 & 0 \\ 0 & 0 & k' \end{bmatrix}$$

If we consider a two-dimensional case ( $x, y$  plane) and let the anisotropy be along  $y$  direction, then equation (2.27) for anisotropic medium will be

$$\frac{\partial^2 \phi}{\partial x^2} + K' \frac{\partial^2 \phi}{\partial y^2} = 0 \quad \dots \quad (2.28)$$

The corresponding variational expression will be

$$\iint \left[ \left( \frac{\partial \phi}{\partial x} \right)^2 + K' \left( \frac{\partial \phi}{\partial y} \right)^2 \right] ds = 0 \quad \dots \quad (2.29)$$

From equation (2.3) the extremum function will be for the  $e$ th element

$$J^e = \frac{1}{2} \iint_{\Omega} \left[ \left( \frac{\partial \phi^e}{\partial x} \right)^2 + K' \left( \frac{\partial \phi^e}{\partial y} \right)^2 \right] dx dy \quad \dots \quad (2.30)$$

Using eqn. (2.14) to (2.18) we can write the element sub-matrix for anisotropic dielectric as

$$\begin{bmatrix} \frac{\partial J^e}{\partial \phi_i} \\ \frac{\partial J^e}{\partial \phi_j} \\ \frac{\partial J^e}{\partial \phi_k} \end{bmatrix} = \begin{bmatrix} b_i^2 + k' c_i^2 & b_i b_j + k' c_i c_j & b_i b_m + k' c_i c_m \\ b_i b_j + k' c_i c_j & b_j^2 + k' c_j^2 & b_j b_m + k' c_j c_m \\ b_i b_m + k' c_i c_m & b_j b_m + k' c_j c_m & b_m^2 + k' c_m^2 \end{bmatrix} \begin{bmatrix} \phi_i \\ \phi_j \\ \phi_m \end{bmatrix} \quad \dots \quad (2.31)$$

Thus a finite element solution for an anisotropic dielectric can be established.



#### 2.4 POTENTIAL DISTRIBUTION IN AN ISOTROPIC DIELECTRIC BETWEEN TWO CIRCULAR PARALLEL PLATES

This will illustrate the form of finite element discretized equations in a two-dimensional boundary value problem. Assuming the structure symmetrical about y its cross-section together with its co-ordinate system is shown in figure 2.1. The corresponding extremum function can be written over element e - as:

$$J^e(\phi) = \frac{1}{2} \iint_e \left[ \left( \frac{\partial \phi^e}{\partial x} \right)^2 + \left( \frac{\partial \phi^e}{\partial y} \right)^2 \right] dx dy.$$

where  $\phi^e$  is the potential over the eth element.

In this case, the upper plate is kept at a certain potential V and the lower plate is maintained at zero potential. The space within these two plates has been divided into 32 triangular elements and 25 nodes. We assume a linear variation of potential over each element and following the procedure discussed earlier, we obtain a set of linear algebraic equations. In this case, corresponding to 25 nodes we get 25 linear algebraic equations. Solution of the above set of linear equations will give the potentials at different nodes. Later on the space has been divided into 64 elements and 45 nodes and the potential

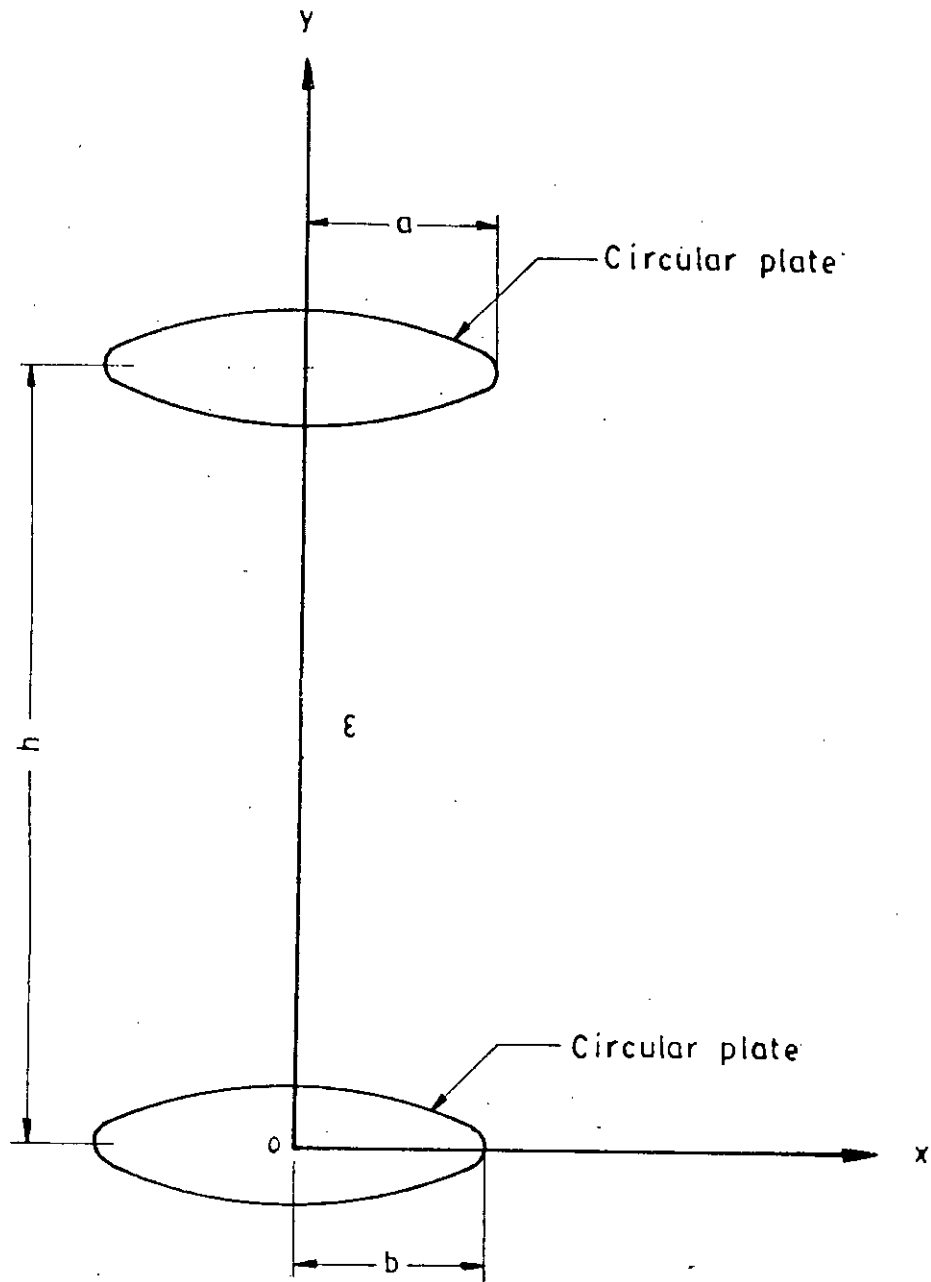


Fig. 2.1. Co-ordinate system of the problem

variation at different levels has been calculated using finite element method. The results are plotted in Fig.2.2. The potential function is symmetrical about the level  $y = h/2$ . That means the potential from the top plate gradually decreases and becomes a constant function of  $x$  at the level  $y = h/2$  where  $\phi = .5v$ . Similarly, the potential from the bottom plate gradually increases to  $\phi = 0.5v$  at the level  $y = h/2$  and becomes a constant function of  $x$ . Thus at  $y = h/2$ ,  $\frac{\partial \phi}{\partial x} = 0$  indicating that at this level no lateral field exists. Rather the field is entirely vertical at the mid level between the two plates. This is expected because the electric lines of forces emanating from the top plate will take turn towards the bottom plate after reaching the mid level. This also indicates that half of the energy is stored in the upper half region and the rest half in the lower half region as is expected in a parallel plate capacitor or in the case of a dipole.

## 2.5 POTENTIAL DISTRIBUTION IN AN ANISOTROPIC DIELECTRIC BETWEEN TWO PARALLEL CIRCULAR PLATES

In this section, finite element method is used in determining the potential distribution in the region between two parallel plates when anisotropic property prevails along  $y$  direction. Following the derivations in section 2.3, numerical results of the potential distribution in the

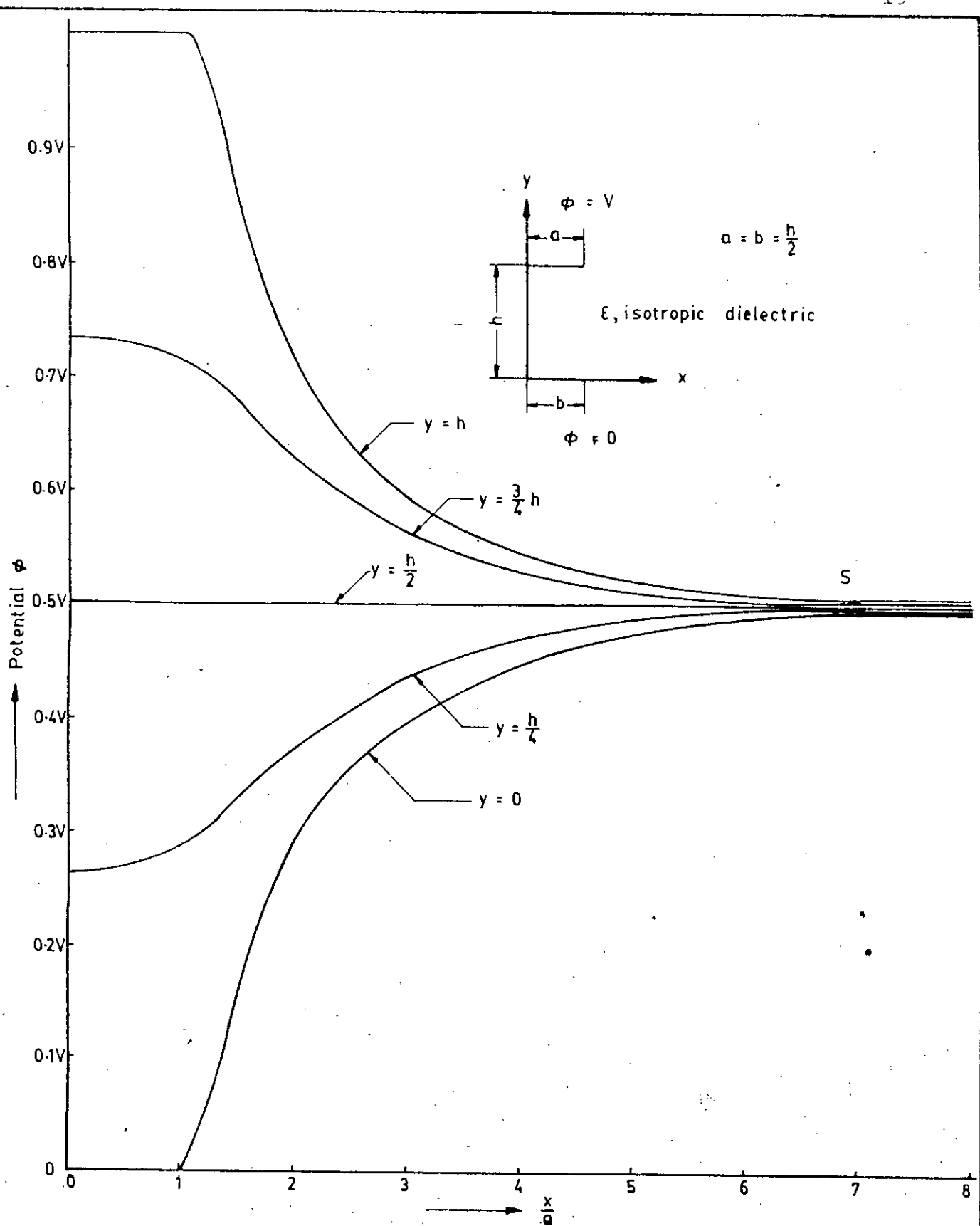


Fig.2.2. Potential distribution between two parallel plates at different insulator heights

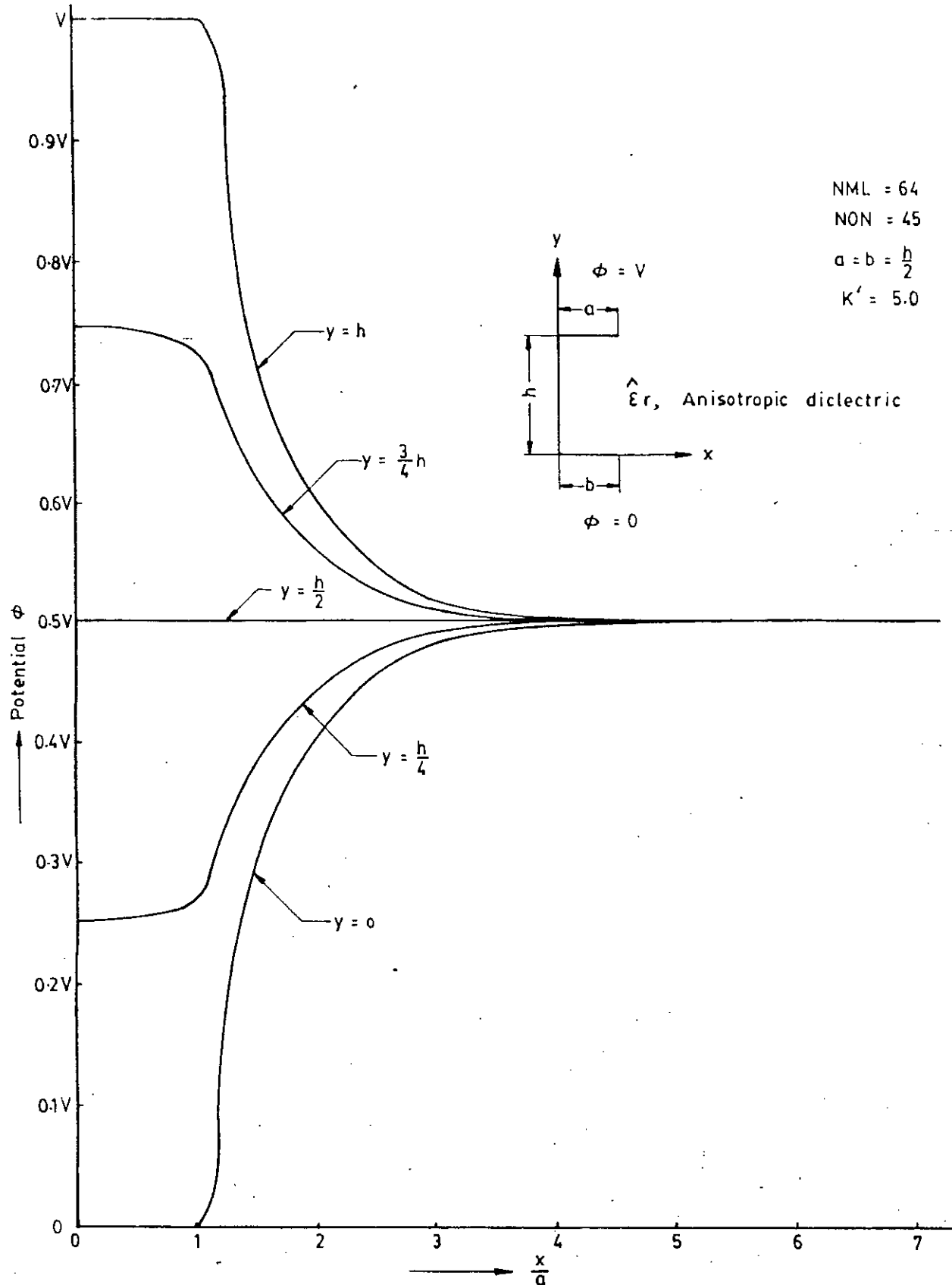


Fig.2.3. Potential distribution between two parallel plates at different insulator heights. For anisotropic medium

anisotropic region are obtained for  $k' = 5.0$  and plotted in Fig. 2.3. The potential function slopes down and slopes up in a faster rate compared to an isotropic dielectric indicating higher electric stress developed in the vertical direction and weaker stress in the lateral direction. This indicates that systems undergoing plastic deformation will experience enhanced stress in the direction of maximum deformation and less stress in the direction of minimum deformation.

## 2.6 DISCUSSION

In the above the finite element method of solving Laplace's equation in isotropic and anisotropic regions is presented in a general manner. An extremum function is defined by linearization of the potential function on each element in such a manner that the conditions of minimum energy is satisfied with the setup of potential at each node. The potential of each node being related to the potentials at other nodes, the minimum energy condition applied at a certain node relates the potentials of all nodes by a linear algebraic equation. With the increase of elements which are triangles for piecewise linearization of the potential function the number of potential nodes and algebraic equations increases. These equations were solved by higher order

matrix inversion using Gaussian elimination method. The numerical data were obtained for potential distribution in isotropic and anisotropic dielectrics between two circular parallel plates. The results are supported by simple physical explanations.

## CHAPTER 3

## ELECTROMECHANICAL STRESS DISTRIBUTION IN INSULATORS

3.1 INTRODUCTION:

The first break-down theory for insulators was the thermal break down theory presented by Wargner [15] in 1922. In this theory the dielectric break-down was discussed in terms of the condition to break-down the thermal balance between Joule heating due to the conduction current and its dissipation. However, there exists low and high temperature region in the temperature dependence of electric strengths of solid dielectric. It is difficult to explain the break-down process in the low temperature region by the thermal break-down theory. Later on electromechanical break-down theory was proposed by Stark [16]. It states that the break-down is caused in insulators by the mechanical deformation due to Maxwell stress under the applied electric field. Allan [17] emphasized the compound nature of stress - electrical, mechanical and thermal for insulation systems.

3.2 ELECTROMECHANICAL STRESS ANALYSIS FOR A DIELECTRIC MEDIUM:

The study of electric stress distribution in and around insulators has been of considerable interests to electrical engineers for designing equipments that operate at very high voltage levels. There is always stress due to the steady state



power frequency voltage. Again, there exists mechanical stress due to mechanical deformation under the applied electric field. The peak stress value in an insulating system is an important parameter because it influences discharge initiation and propagation. There are various numerical techniques that have been used to calculate this stress distribution in and around insulators. With the availability of high speed computers the finite element method has been found to be very useful to solve such type of problems. The electrical stress in insulators is perhaps the easiest to quantify. Because of the geometry of most power system components, the electrical fields that high voltages give rise to are more often than not quite non-uniform. Rapidly changing transient voltages can temporarily cause further extremely non-uniform distribution of stress. In terms of the scalar potential  $\phi$  the electric field intensity  $\bar{E}$  is given by

$$\bar{E} = - \nabla \phi \quad (3.1)$$

where  $\phi$  is the potential distribution.

The theory on Maxwell-Faraday's electro-mechanical stress in 'ether' has been widely discussed by Stratton [22]. We outline below a brief review of the materials covered therein emphasizing their validity for dielectric substances. Let us suppose that a certain bounded region of

space contains charge distributions, but is free of all dielectric. The field is produced in part by the charges within the region and in part by sources which are exterior to it. At every interior point,

Since  $\bar{E} = -\nabla\phi$ , then

$$\nabla \times \bar{E} = 0 \quad (3.2)$$

and 
$$\nabla \cdot \bar{E} = \frac{\rho}{\epsilon_0} \quad (3.3)$$

Let (3.2) be multiplied vectorially by  $\epsilon_0 \bar{E}$ , so we get

$$\epsilon_0 (\nabla \times \bar{E}) \times \bar{E} = 0 \quad (3.4)$$

or

$$\epsilon_0 \begin{vmatrix} \bar{i} & \bar{j} & \bar{k} \\ \frac{\partial E_z}{\partial y} - \frac{\partial E_y}{\partial z} & \frac{\partial E_x}{\partial z} - \frac{\partial E_z}{\partial x} & \frac{\partial E_y}{\partial x} - \frac{\partial E_x}{\partial y} \\ E_x & E_y & E_z \end{vmatrix} = 0$$

Where  $\bar{i}$ ,  $\bar{j}$  and  $\bar{k}$  are unit vectors in the x, y and z directions respectively.

The x component of the vector  $(\nabla \times \bar{E}) \times \bar{E}$  is given by

$$\begin{aligned}
 [(\nabla \times \bar{E}) \times \bar{E}] \cdot \hat{i} &= E_z \left( \frac{\partial E_x}{\partial z} - \frac{\partial E_z}{\partial x} \right) - E_y \left( \frac{\partial E_y}{\partial x} - \frac{\partial E_x}{\partial y} \right) \\
 &= E_z \left( \frac{\partial E_x}{\partial z} - \frac{\partial E_z}{\partial x} \right) - E_y \left( \frac{\partial E_y}{\partial x} - \frac{\partial E_x}{\partial y} \right) + E_x \nabla \cdot \bar{E} - E_x \nabla \cdot \bar{E} \\
 &= E_x \frac{\partial E_x}{\partial x} - E_z \frac{\partial E_z}{\partial x} - E_y \frac{\partial E_y}{\partial x} + E_x \frac{\partial E_y}{\partial y} + E_y \frac{\partial E_x}{\partial y} + E_x \frac{\partial E_z}{\partial z} \\
 &\quad + E_z \frac{\partial E_x}{\partial z} - E_x \nabla \cdot \bar{E} \\
 &= \frac{1}{2} \frac{\partial}{\partial x} E_x^2 - \frac{1}{2} \frac{\partial}{\partial x} E_y^2 - \frac{1}{2} \frac{\partial}{\partial x} E_z^2 + \frac{\partial}{\partial y} (E_x E_y) + \frac{\partial}{\partial z} (E_z E_x) \\
 &\quad - E_x \nabla \cdot \bar{E} \\
 &= \frac{\partial}{\partial x} \left( E_x^2 - \frac{1}{2} E^2 \right) + \frac{\partial}{\partial y} (E_x E_y) + \frac{\partial}{\partial z} (E_z E_x) - E_x \nabla \cdot \bar{E} \quad (3.5)
 \end{aligned}$$

where  $E^2 = E_x^2 + E_y^2 + E_z^2$

Now let  $S_{11} = \epsilon_0 \left( E_x^2 - \frac{1}{2} E^2 \right)$

$$S_{12} = \epsilon_0 E_x E_y$$

$$S_{13} = \epsilon_0 E_x E_z$$

$S_{ij}$  in the above transform constitute the tensor whose components are given in table 3.1. The first three terms on the right side of (3.5) constitute therefore the x component of the divergence of a tensor  $\hat{S}$ . The remaining components are calculated from the y and z components of  $\epsilon_0 (\nabla \times \bar{E}) \times \bar{E}$ , such that we are led to the identity

$$\epsilon_0 (\nabla \times \bar{E}) \times \bar{E} = \nabla \cdot \hat{S} \bar{I} - \epsilon_0 \bar{E} \nabla \cdot \bar{E} \quad \dots \quad (3.6)$$

where  $\bar{I}$  is the unit column vector

$$\bar{I} = \begin{bmatrix} i \\ j \\ k \end{bmatrix} \quad \dots \quad (3.7)$$

Table 3.1: Components  $S_{ij}$  of the tensor  $\hat{S}$  in free space

j/k	1	2	3
1	$\epsilon_0 E_x^2 - \frac{\epsilon_0}{2} E^2$	$\epsilon_0 E_x E_y$	$\epsilon_0 E_x E_z$
2	$\epsilon_0 E_y E_x$	$\epsilon_0 E_y^2 - \frac{\epsilon_0}{2} E^2$	$\epsilon_0 E_y E_z$
3	$\epsilon_0 E_z E_x$	$\epsilon_0 E_z E_y$	$\epsilon_0 E_z^2 - \frac{\epsilon_0}{2} E^2$

If stationary charge distribution is considered, the fields are then independent of time, then taking help of equation (3.3) , equation (3.6) reduces to

$$\nabla \cdot \hat{S}\bar{I} = \bar{E}\rho \quad (3.8)$$

Equation (3.8) is a relation through which the forces exerted on elements of charge at any point in empty space is expressed in terms of the vector  $\bar{E}$ . As the charge density  $\rho$  is in coulomb/m<sup>3</sup>, the force distribution given by the right hand side of (3.8) will be in Newton/m<sup>3</sup>. Let us now integrate the identity (3.8) over a volume  $v$ . The integral of the divergence of the tensor throughout  $v$  is equal to the integral of a vector over the surface bounding  $v$ . Let  $\bar{n}$  be the unit outward normal at a point on the bounding surface. Then the total force exerted on the charges enclosed is given by

$$\bar{F} = \int_v \nabla \cdot \hat{S}\bar{I} \, dv = \int_v \bar{E}\rho \, dv \quad \dots \quad (3.9)$$

By divergence theorem

$$\bar{F} = \oint_a (\hat{S}\bar{I}) \cdot \bar{n} \, da = \int_v \bar{E}\rho \, dv \quad \dots \quad (3.10)$$

Thus the quantity  $(\hat{S}\bar{I}) \cdot \bar{n}$  comes out in the form of force per unit area or as a mechanical stress. That means  $(\hat{S}\bar{I}) \cdot \bar{n}$  represents a mechanical stress developed with application of the electric stress  $\bar{E}$ . Any neutral body between an electric potential difference will experience such mechanical stress in the form of compression or tension. For free space between the two plates the mechanical stress will work on the potential plates only. In light of the above discussion the analysis for an isotropic dielectric medium surrounding the charges can be carried out in the following manner.

Let us multiply eqn. (3.6) by the relative permittivity  $\epsilon_r$  of the dielectric so that

$$\epsilon_0 (\nabla \times \bar{E}) \times \epsilon_r \bar{E} = \epsilon_r \nabla \cdot \hat{S}\bar{I} - \bar{E} \nabla \cdot \epsilon_0 \epsilon_r \bar{E} = 0 \quad (3.11)$$

For a dielectric since  $\bar{D} = \epsilon_0 \epsilon_r \bar{E}$ , then (3.11) can be written as

$$\epsilon_r \nabla \cdot \hat{S}\bar{I} = \bar{E} \nabla \cdot \bar{D} \quad \dots \quad (3.12)$$

Now for a dielectric medium

$$\bar{D} = \bar{D}_0 + \bar{P} \quad \dots \quad (3.13)$$

where  $\bar{P}$  is the amount of electric polarization in the dielectric and  $\bar{D}_0 = \epsilon_0 \bar{E}$  is the unpolarized portion of the electric flux density  $\bar{D}$ . Then

$$\nabla \cdot \bar{D} = \nabla \cdot \bar{D}_0 + \nabla \cdot \bar{P}$$

The unpolarized flux density  $\bar{D}_0$  links the charges and  $\bar{P}$  is the portion of the flux density absorbed in the region in polarizing the dipole moments of the dielectric. On the charged regions  $\bar{P} = 0$  so that

$$\nabla \cdot \bar{D} = \nabla \cdot \bar{D}_0 = \rho \quad \dots \quad (3.14)$$

In the dielectric region  $\rho = 0$ , hence  $\nabla \cdot \bar{D}_0 = 0$

$$\text{so that} \quad \nabla \cdot \bar{D} = \nabla \cdot \bar{P} \quad \dots \quad (3.15)$$

Thus equation (3.12) can be written as for charged regions

$$\epsilon_r \nabla \cdot \hat{S}\bar{I} = E\rho \quad \dots \quad (3.16)$$

for dielectric region

$$\epsilon_r \nabla \cdot \hat{S}\bar{I} = E\nabla \cdot \bar{P} \quad \dots \quad (3.17)$$

Hence the forces in the charged and dielectric regions are given respectively as

$$\bar{F} = \epsilon_r \oint_a \hat{S}\bar{I} \cdot \bar{n} da = \int_v E \rho dv \quad \dots \quad (3.18)$$

$$\bar{F} = \epsilon_r \oint_a \hat{S}\bar{I} \cdot \bar{n} da = \int_v E \nabla \cdot \bar{P} \quad \dots \quad (3.19)$$

Identical form of the left hand sides of eqns. (3.18) and (3.19) indicates that the electromechanical force is continuous indicating that in the dielectric region  $\rho$  is replaceable by the hypothetical charge density  $\nabla \cdot \bar{P}$ . Moreover in the present case all stress elements will be  $\epsilon_r$  times greater than those for free space.

Equation (3.19) does not state that the volume force  $F$  is maintained in equilibrium by the force  $\epsilon_r \hat{S}\bar{I} \cdot \bar{n}$  distributed over the surface. The equilibrium must be established with mechanical forces of some other type and in fact, a charge distribution can not be maintained in static equilibrium under the action of electrical forces alone. For equilibrium the determinant of the stress tensor must vanish, i.e.

$$\epsilon_r \begin{vmatrix} \epsilon_0 (E_x^2 - \frac{1}{2} E^2) - \lambda & \epsilon_0 E_x E_y & \epsilon_0 E_x E_z \\ \epsilon_0 E_y E_x & \epsilon_0 (E_y^2 - \frac{1}{2} E^2) - \lambda & \epsilon_0 E_y E_z \\ \epsilon_0 E_z E_x & \epsilon_0 E_z E_y & \epsilon_0 (E_z^2 - \frac{1}{2} E^2) - \lambda \\ \dots & & \dots \end{vmatrix} = 0 \quad (3.20)$$



When expanded and reduced by taking account of the relation  $E_x^2 + E_y^2 + E_z^2 = E^2$ ,

Eqn . (3.20) proves equivalent to

$$8\lambda^3 + 4E^2\lambda^2 - 2E^4\lambda\epsilon_0^2 - \epsilon_0^3 E^6 = 0 \quad \dots \quad (3.21)$$

The roots of (3.21) are, therefore,

$$\lambda_a = \frac{\epsilon_0}{2} E^2, \quad \lambda_b = \lambda_c = -\frac{\epsilon_0}{2} E^2 \quad \dots \quad (3.22)$$

It is evident from (3.22) that the stress quadratic has an axis of symmetry. Let  $\bar{n}^{(a)}$  be a unit vector fixing the direction of the principal axis associated with  $\lambda_a$ . The components of  $\bar{n}^{(a)}$  with respect to an arbitrary reference system must satisfy-

$$\begin{aligned} (E_x^2 - E^2) n_x^{(a)} + E_x E_y n_y^{(a)} + E_x E_z n_z^{(a)} &= 0 \\ E_y E_x n_x^{(a)} + (E_y^2 - E^2) n_y^{(a)} + E_y E_z n_z^{(a)} &= 0 \quad \dots \quad (3.23) \\ E_z E_x n_x^{(a)} + E_z E_y n_y^{(a)} + (E_z^2 - E^2) n_z^{(a)} &= 0 \end{aligned}$$

From the theory of homogeneous equations it is known that the ratios of unknowns  $n_x^{(a)}$ ,  $n_y^{(a)}$ ,  $n_z^{(a)}$  are the ratios of the minors of the determinant of the system, whence it is clear

from (3.23) that

$$n_x^{(a)} : n_y^{(a)} : n_z^{(a)} = E_x : E_y : E_z \quad \dots \quad (3.24)$$

The major axis of the mechanical stress quadratic at any point in the field is directed along the vector  $\bar{E}$  at that point. The stress transmitted across an element of surface whose normal is oriented in this direction is a simple tension,

$$\bar{t}^{(a)} = \frac{\epsilon_0 \epsilon_r}{2} E^2 \bar{n}^{(a)} \quad \dots \quad (3.25)$$

The stress across any element of surface containing the vector  $\bar{E}$  - i.e., an element whose normal is at right angles to the lines of force is also normal but negative, and corresponds therefore to a compression,

$$\bar{t}^{(b)} = -\frac{\epsilon_0 \epsilon_r}{2} E^2 \bar{n}^{(b)}, \quad \bar{t}^{(c)} = -\frac{\epsilon_0 \epsilon_r}{2} E^2 \bar{n}^{(c)} \quad \dots \quad (3.26)$$

Now let us write the mechanical stress at any point as

$$\bar{t} = \epsilon_r \hat{S} \bar{I} \cdot \bar{n} \quad \dots \quad (3.27)$$

Then

$$\begin{aligned} t_x &= \epsilon_r (S_{11} n_x + S_{12} n_y + S_{13} n_z) \\ t_y &= \epsilon_r (S_{21} n_x + S_{22} n_y + S_{23} n_z) \\ t_z &= \epsilon_r (S_{31} n_x + S_{32} n_y + S_{33} n_z) \end{aligned} \quad \dots \quad (3.28)$$

Where  $n_x, n_y$  and  $n_z$  are components of the normal  $\bar{n}$  along  $x, y$  and  $z$  directions respectively. Suppose, the normal  $\bar{n}$  of a surface element in the field is oriented in an arbitrary direction. Let the  $z$  axis of a co-ordinate system located at the point in question be drawn parallel to  $\bar{E}$  and the  $x$ -axis be perpendicular to the plane through  $\bar{E}$  and  $\bar{n}$ . Let the angle made by  $\bar{n}$  with  $\bar{E}$  be  $\theta$ . Then

$$E_x = E_y = 0 \quad |\bar{E}| = E_z$$

$$n_x = 0, \quad n_y = \sin\theta \text{ and } n_z = \cos\theta,$$

The stress components by Table 3.1 are:

$$t_x = 0, \quad t_y = -\frac{\epsilon_0 \epsilon_r}{2} E^2 \sin\theta, \quad t_z = \frac{\epsilon_0 \epsilon_r}{2} E^2 \cos\theta$$

Hence the angle of the stress with this electric field  $\bar{E}$  is given by

$$\alpha = \tan^{-1} \frac{t_y}{t_z} = -\theta \quad \dots \quad (3.29)$$

The absolute value of the mechanical stress transmitted across any surface element, whatever its orientation, is therefore,

$$|t| = \frac{\epsilon_0 \epsilon_r}{2} E^2 = \frac{1}{2} \bar{D} \cdot \bar{E} \quad \dots \quad (3.30)$$

Furthermore  $\bar{t}$  lies in the plane of  $\bar{E}$  and  $\bar{n}$  in a direction such that  $\bar{E}$  bisects the angle between  $\bar{n}$  and  $\bar{t}$  as illustrated in Fig. 3.1.

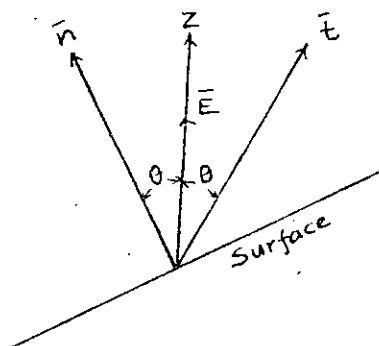


Fig. 3.1 : Relation of tension  $\bar{t}$  transmitted across an element of surface in an electrostatic field to the field intensity  $\bar{E}$ .

### 3.3 ELECTROMECHANICAL STRESS DISTRIBUTION IN AN ISOTROPIC DIELECTRIC BETWEEN TWO PARALLEL CIRCULAR PLATES.

In order to obtain the electric stress distribution between two parallel plates by finite element method let us first consider a general triangular element having nodes  $i, j, m$ .  $\phi_i$ ,  $\phi_j$  and  $\phi_m$  being the corresponding node potentials.

The electric field components are given by

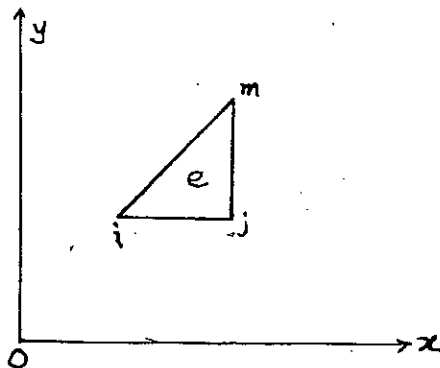


Fig. 3.2: A generalized triangular element.

$$E_x = - \frac{\partial \phi^e}{\partial x} \quad \text{and} \quad E_y = - \frac{\partial \phi^e}{\partial y}$$

where  $\phi^e$  is the potential function over an element. From equation (2.9) we have the potential variation over the eth element as

$$\phi^e(x, y) = \frac{1}{2A} \left[ (a_i + b_i x + c_i y) \phi_i^{(e)} + (a_j + b_j x + c_j y) \phi_j^{(e)} + (a_m + b_m x + c_m y) \phi_m^{(e)} \right]$$

where  $A = \frac{1}{2} \begin{vmatrix} 1 & x_i & y_i \\ 1 & x_j & y_j \\ 1 & x_m & y_m \end{vmatrix}$

$$\text{Hence } E_x = - \frac{1}{2A} \left[ b_i \phi_i^{(e)} + b_j \phi_j^{(e)} + b_m \phi_m^{(e)} \right] \quad \dots \quad (3.31)$$

$$E_y = - \frac{1}{2A} \left[ c_i \phi_i^{(e)} + c_j \phi_j^{(e)} + c_m \phi_m^{(e)} \right] \quad \dots \quad (3.32)$$

where the values of  $a_i, b_i, c_i$  are given by eqn. no. (2.10).

Applying the above two equations for electric stress over each element, electric stress distribution over the entire region can be calculated. For determining the corresponding mechanical stresses developed at different levels between the two parallel plates, let us consider the unit normal  $\bar{n}$  in the y-direction. So that  $n_x = 0$  and  $n_z = 0$ .

Hence by using the elements of stress tensor given in Table 3.1, the mechanical stress components are given by

$$t_x = S_{12} = \epsilon_0 \epsilon_r E_y E_x \quad \dots \quad (3.33)$$

$$t_y = S_{22} = \frac{1}{2} \epsilon_0 \epsilon_r (E_y^2 - E_x^2) \quad \dots \quad (3.34)$$

The magnitude of the resultant stress is given by

$$\begin{aligned} |t| &= \sqrt{t_x^2 + t_y^2} \\ &= \epsilon_0 \epsilon_r \sqrt{\left(\frac{E_x^2 - E_y^2}{2}\right)^2 + E_x^2 E_y^2} \\ &= \frac{\epsilon_0 \epsilon_r}{2} (E_x^2 + E_y^2) = \frac{\epsilon_0 \epsilon_r}{2} E^2 \\ &= \frac{1}{2} \bar{D} \cdot \bar{E} \quad \dots \quad (3.35) \end{aligned}$$

The angle  $\theta_m$  of the mechanical stress produced with x-axis is given by

$$\begin{aligned} \theta_m &= \tan^{-1} \frac{t_y}{t_x} \\ &= \tan^{-1} \frac{E_x E_y}{E_y^2 - E_x^2} \end{aligned}$$

In terms of the angle of electrical stress  $\theta_e = \tan^{-1} \frac{E_y}{E_x}$

We get

$$\theta_m = 2\theta_e - 90^\circ \quad \dots \quad (3.36)$$

It can be readily checked that the electric field vector bisects the angle between the normal  $\bar{n}$  and the mechanical stress  $\bar{t}$ , a fact that has been pointed out in section 3.2.

Fig. 3.3 and 3.4 represent respectively the magnitudes of electrical and mechanical stress distributions calculated by finite element method at different levels of an isotropic dielectric between two circular parallel plates of identical size. The corresponding variation of angles of these stress vectors are given in table 3.2. Both types of stresses are maximum at the edges of the top and the bottom plates. On the potential plates the mechanical stress produces a tension which is balanced by the compressive electric force. At the edges of the top plate a strong compressive mechanical stress is developed in the lateral direction and at the edges of the bottom plate the resulting stress is a strong tension both in lateral and vertical directions. With the increase of distance from the potential plates the electromechanical stress decreases rapidly. The mid-level at  $y = \frac{h}{2}$  is subjected to equal and opposite electromechanical forces in the vertical. However, shear

forces will develop at this level in the lateral direction. Because the lateral mechanical stresses above and below this level are oppositely directed. Under critical circumstances the electric force between the two plates may not be sufficient to save the dielectric from lateral fracture due to these lateral shear forces. While the upper portion of the dielectric will tend to move to the left, the lower portion will tend to move to the right due to the antiparallel lateral stresses in the two portions of the dielectric. These phenomena can be clearly visualized from the variation of stress angles given in table 3.2. Perhaps this is the reason why capacitors burst under intolerable voltages. Fig. 3.5 and 3.6 illustrate the electromechanical stress distribution for unequal sizes of the potential plates. Stresses are invariably maximum at the edges of plates. Distributions of electrical and mechanical stress angles for this case are shown in Table 3.3. Variation of angles are almost same as the former case.



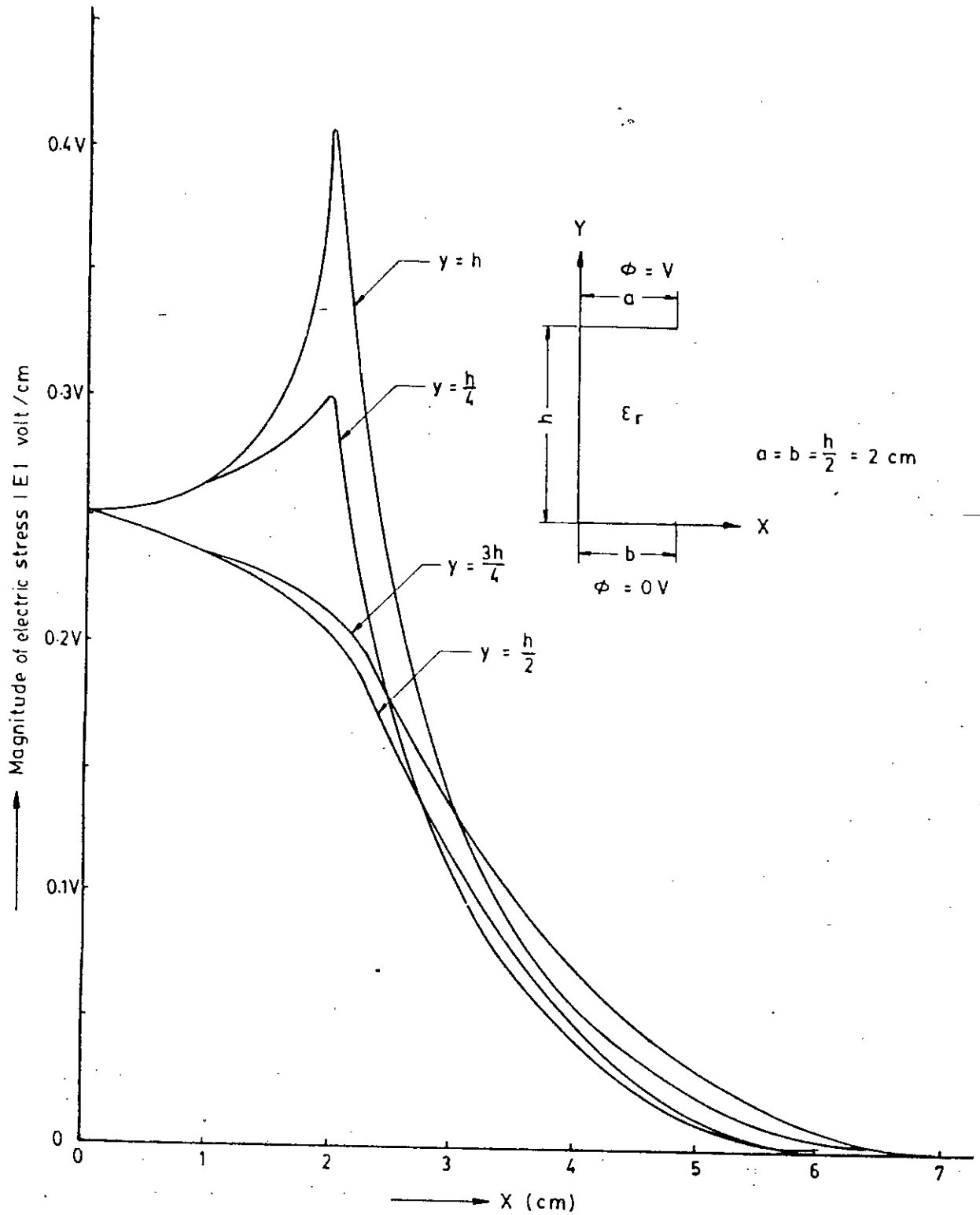


Fig. 3.3 Electric stress distribution between two parallel circular plates in an isotropic dielectric

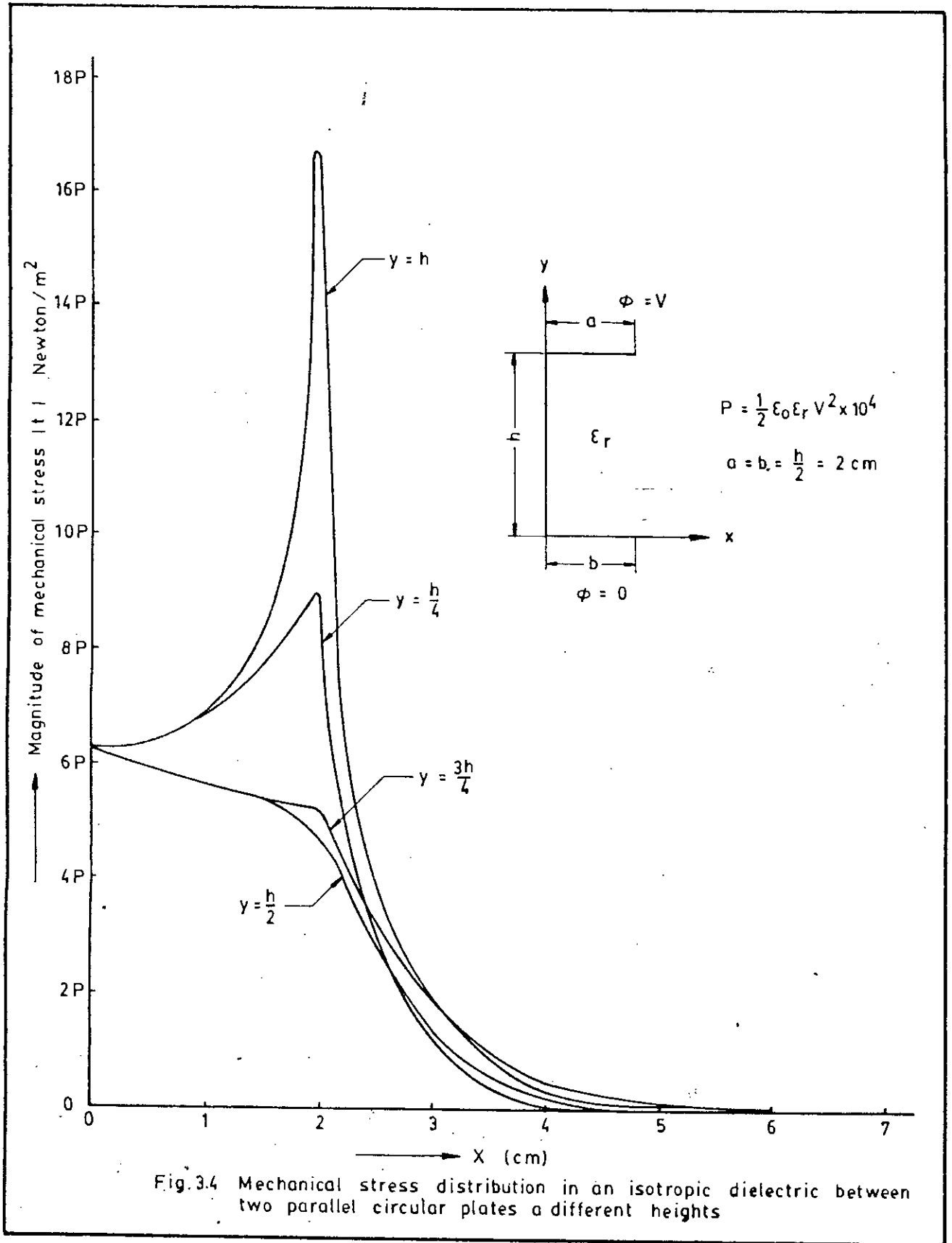


TABLE 3.2: Variation of Electrical and Mechanical stress angles with the horizontal plane at different levels in an isotropic dielectric between two circular parallel plates.  $a=b=h/2 = 2$  cm.

$x$ $y$ (cm)	0	1	2	3	4	5	6	7	
4	$\theta_e$	$-90^\circ$	$-90^\circ$	$-44.41^\circ$	$-37.29^\circ$	$-33.05^\circ$	$-31.57^\circ$	$-33.82^\circ$	$-52.49^\circ$
	$\theta_m$	$+90^\circ$	$+90^\circ$	$-178.82^\circ$	$-164.58^\circ$	$-156.10^\circ$	$-153.14^\circ$	$-157.64^\circ$	$-194.98^\circ$
3	$\theta_e$	$-88.89^\circ$	$-84.17^\circ$	$-66.48^\circ$	$-63.70^\circ$	$-62.98^\circ$	$-63.30^\circ$	$-65.99^\circ$	$-77.32^\circ$
	$\theta_m$	$-267.78^\circ$	$-258.34^\circ$	$-222.96^\circ$	$-217.40^\circ$	$-215.96^\circ$	$-216.60^\circ$	$-221.98^\circ$	$-244.64^\circ$
2	$\theta_e$	$-90.00^\circ$	$-90^\circ$	$-90^\circ$	$-90^\circ$	$-90^\circ$	$-90^\circ$	$-90^\circ$	$-90^\circ$
	$\theta_m$	$+90.00^\circ$	$+90^\circ$	$+90^\circ$	$+90^\circ$	$+90^\circ$	$+90^\circ$	$+90^\circ$	$+90^\circ$
1	$\theta_e$	$-91.07^\circ$	$-95.39^\circ$	$-108.22^\circ$	$-124.4^\circ$	$-133.86^\circ$	$-137.57^\circ$	$-135.9^\circ$	$-118.19^\circ$
	$\theta_m$	$+87.86^\circ$	$+79.22^\circ$	$+53.56^\circ$	$+21.20^\circ$	$+2.28^\circ$	$-5.14^\circ$	$-1.8^\circ$	$+33.62^\circ$
0	$\theta_e$	$-90^\circ$	$-90^\circ$	$-163.20^\circ$	$-164.21^\circ$	$-164.58^\circ$	$-164.02^\circ$	$-160.13^\circ$	$-134.97^\circ$
	$\theta_m$	$+90^\circ$	$+90^\circ$	$-56.4^\circ$	$-58.42^\circ$	$-59.16^\circ$	$-58.04^\circ$	$-50.26^\circ$	$+0.06^\circ$

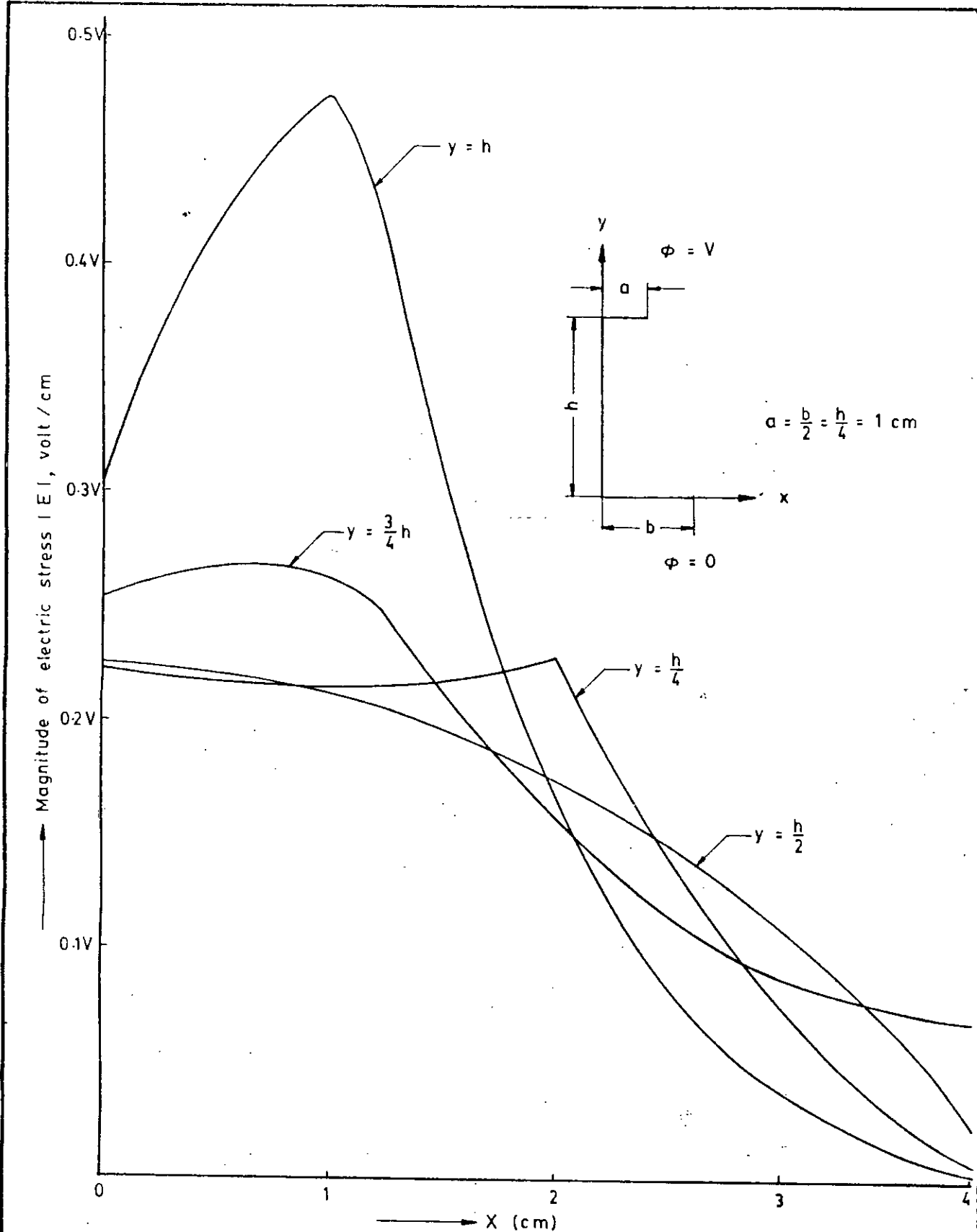


Fig. 3.5. Electric stress distribution between two unequal parallel circular plates

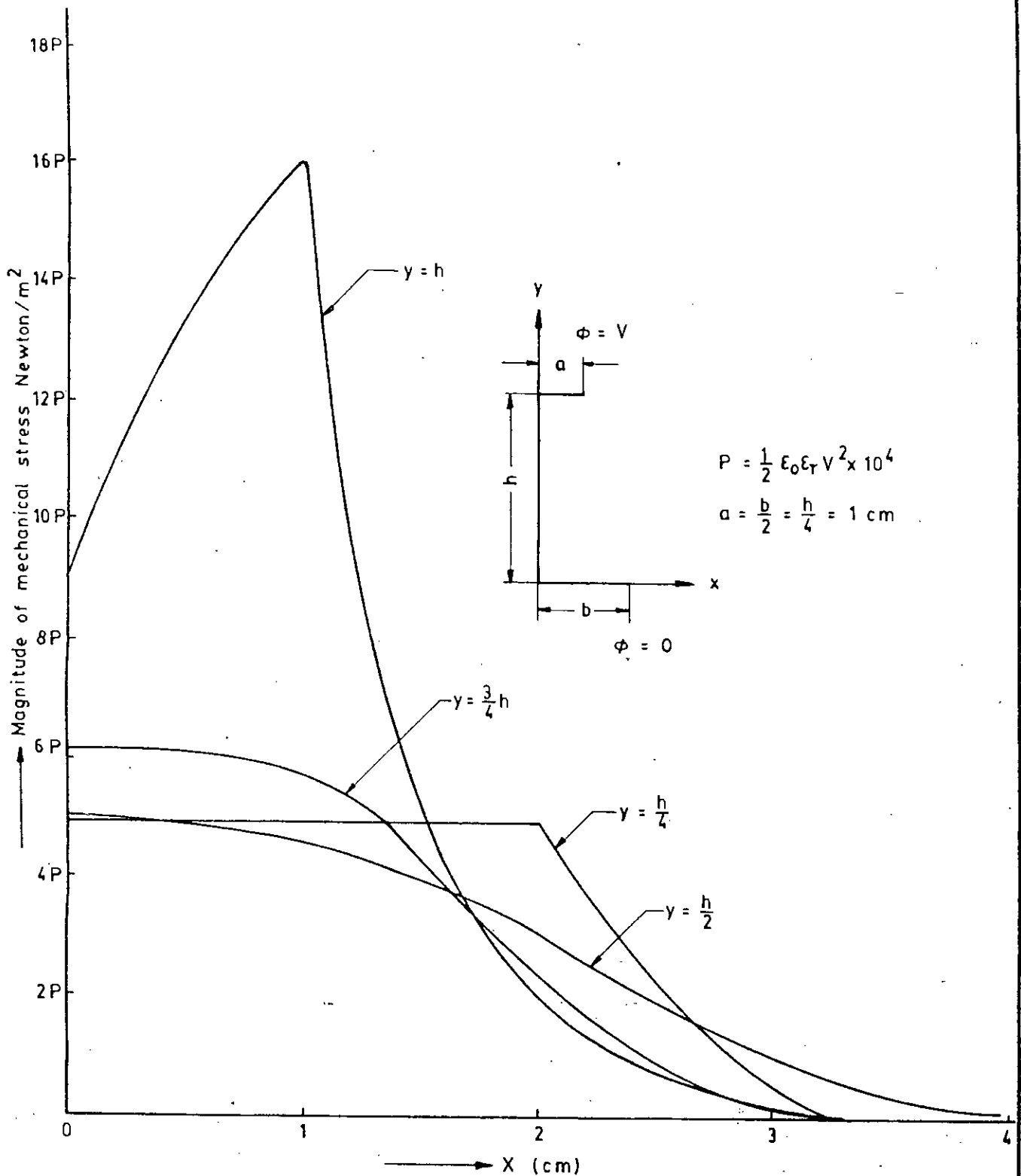


Fig.3.6 Mechanical stress distribution between two unequal circular parallel plates

Table 3.3: Variation of electrical and mechanical stress angles at different points between two unequal parallel circular plates in isotropic dielectric

$$a = \frac{b}{2} = \frac{h}{4} = 1 \text{ cm.}$$

$\begin{matrix} x \\ y \\ \text{(cm)} \end{matrix}$	0	1	2	3	4	5	6	7
4 $\theta_e$	$-90^\circ$	$-43.2^\circ$	$-35.28^\circ$	$-31.08^\circ$	$-29.58^\circ$	$-29.78^\circ$	$-32.95^\circ$	$-52.20^\circ$
$\theta_m$	$+90^\circ$	$-176.4^\circ$	$-160.56^\circ$	$-152.16^\circ$	$-149.16^\circ$	$-147.56^\circ$	$-155.9^\circ$	$-194^\circ$
3 $\theta_e$	$-83.68^\circ$	$-61.88^\circ$	$-60.45^\circ$	$-60.82^\circ$	$-61.45^\circ$	$-62.48^\circ$	$-65.57^\circ$	$-77.19^\circ$
$\theta_m$	$+102.64^\circ$	$+146.24^\circ$	$149.1^\circ$	$148.4^\circ$	$147.1^\circ$	$+145^\circ$	$+139^\circ$	$+116^\circ$
2 $\theta_e$	$-86.63^\circ$	$-80.05^\circ$	$-84.69^\circ$	$-86.72^\circ$	$-87.99^\circ$	$-88.82^\circ$	$-89.36^\circ$	$-89.79^\circ$
$\theta_m$	$+96.74^\circ$	$+110^\circ$	$+100.62^\circ$	$96.56^\circ$	$94^\circ$	$92.36^\circ$	$91.28^\circ$	$90.42^\circ$
1 $\theta_e$	$-89.67^\circ$	$-91.53^\circ$	$-105.54^\circ$	$-120.98^\circ$	$-131.84^\circ$	$-135.8^\circ$	$-134.8^\circ$	$-117.7^\circ$
$\theta_m$	$90.66^\circ$	$86.94^\circ$	$58.92^\circ$	$28.04^\circ$	$6.32^\circ$	$-1.6^\circ$	$0.4^\circ$	$34.6^\circ$
0 $\theta_e$	$-90^\circ$	$-90^\circ$	$-162.85^\circ$	$-163.89^\circ$	$-164.37^\circ$	$-163.89^\circ$	$-160.1^\circ$	$-134.98^\circ$
$\theta_m$	$+90^\circ$	$+90^\circ$	$-55.7^\circ$	$-57.78^\circ$	$-58.74^\circ$	$-57.78^\circ$	$-50.2^\circ$	$+0.04^\circ$

### 3.4 ELECTROMECHANICAL STRESS DISTRIBUTION IN AN ANISOTROPIC DIELECTRIC BETWEEN TWO CIRCULAR PARALLEL PLATES.

In section 3.2 the mechanical stress tensor developed from electric forces has been derived for an isotropic dielectric. Let us now extend the analysis for anisotropic dielectric of which the anisotropy is characterized by the relative permittivity tensor.

$$\hat{\epsilon}_r = \epsilon_r \begin{bmatrix} 1 & 0 & 0 \\ 0 & 1 & 0 \\ 0 & 0 & k' \end{bmatrix} \quad (3.37)$$

we have

$$\bar{E} = - \nabla \phi \quad (3.38)$$

$$\text{Then } \nabla \times \bar{E} = 0 \quad (3.39)$$

For obtaining the electromechanical stress tensor let us study the identity

$$(\nabla \times \bar{E}) \times \hat{\epsilon}_r \bar{E} = \begin{vmatrix} \bar{i} & \bar{j} & \bar{k} \\ \frac{\partial E_z}{\partial y} - \frac{\partial E_y}{\partial z} & \frac{\partial E_x}{\partial z} - \frac{\partial E_z}{\partial x} & \frac{\partial E_y}{\partial x} - \frac{\partial E_x}{\partial y} \\ \epsilon_r E_x & \epsilon_r E_y & \epsilon_r k' E_z \end{vmatrix}$$

x, y and z components of this vector are respectively

$$\left[ (\nabla \times \bar{E}) \times \hat{\epsilon}_r \bar{E} \right] \cdot \bar{i} = \epsilon_r \left[ \frac{\partial}{\partial x} (E_x^2 - \frac{1}{2} E'^2) + \frac{\partial}{\partial y} (E_y E_x) \right. \\ \left. + \frac{\partial}{\partial z} (k' E_z E_x) \right] - E_x \nabla \cdot \hat{\epsilon}_r \bar{E}$$

$$\left[ (\nabla \times \bar{E}) \times \hat{\epsilon}_r \bar{E} \right] \cdot \bar{j} = \epsilon_r \left[ \frac{\partial}{\partial x} (E_x E_y) + \frac{\partial}{\partial y} (E_y^2 - \frac{1}{2} E'^2) \right. \\ \left. + \frac{\partial}{\partial z} (k' E_y E_z) \right] - E_y \nabla \cdot \hat{\epsilon}_r \bar{E}$$

$$\left[ (\nabla \times \bar{E}) \times \hat{\epsilon}_r \bar{E} \right] \cdot \bar{k} = \epsilon_r \left[ \frac{\partial}{\partial x} (E_x E_z) + \frac{\partial}{\partial y} (E_y E_z) \right. \\ \left. + \frac{\partial}{\partial z} (k' E_z^2 - \frac{1}{2} E'^2) \right] - E_z \nabla \cdot \hat{\epsilon}_r \bar{E}$$

where  $E'^2 = E_x^2 + E_y^2 + k' E_z^2$

Thus we can write

$$\epsilon_0 (\nabla \times \bar{E}) \times \hat{\epsilon}_r \bar{E} = \nabla \cdot \hat{S}' \bar{I} - \epsilon_0 \bar{E} \nabla \cdot \hat{\epsilon}_r \bar{E} = 0 \quad \dots (3.40)$$

where  $\hat{S}'$  is the tensor

$$\hat{S}' = \begin{bmatrix} S'_{11} & S'_{12} & S'_{13} \\ S'_{21} & S'_{22} & S'_{23} \\ S'_{31} & S'_{32} & S'_{33} \end{bmatrix}$$



and  $\bar{I}$  is the unit column vector defined in eqn. (3.7).

The elements of the tensor  $\hat{S}'$  are given by

$$S'_{11} = \epsilon_0 \epsilon_r (E_x^2 - \frac{1}{2} E'^2) , \quad S'_{12} = \epsilon_0 \epsilon_r E_y E_x ,$$

$$S'_{13} = \epsilon_0 \epsilon_r k' E_z E_x$$

$$S'_{21} = \epsilon_0 \epsilon_r E_x E_y , \quad S'_{22} = \epsilon_0 \epsilon_r (E_y^2 - \frac{1}{2} E'^2) , \quad S'_{23} = \epsilon_0 \epsilon_r k' E_y E_z$$

$$S'_{31} = \epsilon_0 \epsilon_r E_x E_z , \quad S'_{32} = \epsilon_0 \epsilon_r E_y E_z , \quad S'_{33} = \epsilon_0 \epsilon_r (k' E_z^2 - \frac{1}{2} E'^2)$$

By taking volume integral over eqn. (3.40)

We get

$$\int_V \nabla \cdot \hat{S}' \bar{I} \, dv = \int_V \bar{E} \nabla \cdot \epsilon_0 \hat{\epsilon}_r \bar{E} \, dv \quad \dots \quad (3.41)$$

By divergence theorem

$$\oint_a \hat{S}' \bar{I} \cdot \bar{n} \, da = \int_V \bar{E} \nabla \cdot \epsilon_0 \hat{\epsilon}_r \bar{E} \, dv$$

$$\text{since } \bar{D} = \epsilon_0 \hat{\epsilon}_r \bar{E} = \epsilon_0 \bar{E} + \bar{P}$$

where  $\bar{P}$  is the polarization in the dielectric.

$$\text{Then } \nabla \cdot \bar{D} = \nabla \cdot \epsilon_0 \hat{\epsilon}_r \bar{E} = \nabla \cdot \bar{D}_0 + \nabla \cdot \bar{P}$$

Hence (3.41) can be written as

$$\oint_a \hat{S}' \bar{I} \cdot \bar{n} da = \int_v \bar{E} (\rho + \nabla \cdot \bar{P}) dv \quad \dots \quad (3.42)$$

On the charged region  $\bar{P} = 0$  so that

$$\oint_a \hat{S}' \bar{I} \cdot \bar{n} da = \int_v \bar{E} \rho dv$$

Outside the charged region  $\rho = 0$ , then

$$\oint_a \hat{S}' \bar{I} \cdot \bar{n} da = \int_v \bar{E} \nabla \cdot \bar{P} dv \quad \dots \quad (3.43)$$

The right hand side of this equation represents the force exerted on the dipole moments. From the left hand side it is evident that  $\hat{S}'$  represents the mechanical stress tensor. The mechanical stress  $\bar{t}$  is given by

$$\bar{t} = \hat{S}' \bar{I} \cdot \bar{n} \quad \dots \quad (3.44)$$

Let us now apply the theory to the problem of an anisotropic dielectric between two parallel circular plates. Considering the axis of the plates along the z- direction experiencing the effect of anisotropy we can from symmetry analyze the problem in the y-z system. Let the unit normal  $\bar{n}$  be parallel to the z-axis being perpendicular to the potential plates. Then  $E_x = 0$ ,  $n_x = 0$ ,  $n_y = 0$  and  $n_z = 1$

Thus the y- component of the stress becomes

$$t_y = S'_{23} = \epsilon_0 \epsilon_r k' E_y E_z \quad \dots \quad (3.45)$$

$$t_z = S'_{33} = \epsilon_0 \epsilon_r (k'E_z^2 - \frac{1}{2} E'^2) \quad \dots \quad (3.46)$$

The resulting stress is given by

$$\begin{aligned} |t| &= \sqrt{t_y^2 + t_z^2} = \epsilon_0 \epsilon_r \sqrt{k'E_y^2 E_z^2 + (k'E_z^2 - \frac{1}{2} E'^2)^2} \\ &= \epsilon_0 \epsilon_r \sqrt{k'^2 E_y^2 E_z^2 + \frac{(k'E_z^2 - E_y^2)^2}{2}} \\ &= \frac{\epsilon_0}{2} \epsilon_r \sqrt{(E_y^2 + k'E_z^2)^2} \\ &= \frac{\epsilon_0}{2} \epsilon_r (E_y^2 + k'E_z^2) = \frac{1}{2} \epsilon_0 \hat{\epsilon}_r \bar{E} \cdot \bar{E} \quad \dots \quad (3.47) \end{aligned}$$

Thus for linear isotropic and anisotropic dielectrics the magnitude of the electro-mechanical stress can be calculated readily from

$$|t| = \frac{1}{2} \bar{D} \cdot \bar{E} \quad \dots \quad (3.48)$$

The angle of the stress with the y-axis is given by

$$\begin{aligned} \theta_m &= \tan^{-1} \frac{t_z}{t_y} \\ &= \tan^{-1} \frac{k'E_z^2 - E_y^2}{2k'E_y E_z} \end{aligned}$$

In terms of the angle of the electric field  $\theta_e = \tan^{-1} \frac{E_z}{E_y}$

We get

$$\theta_m = \tan^{-1} \frac{k' \tan^2 \theta_e - 1}{2k' \tan \theta_e} \quad \dots \quad (3.49)$$

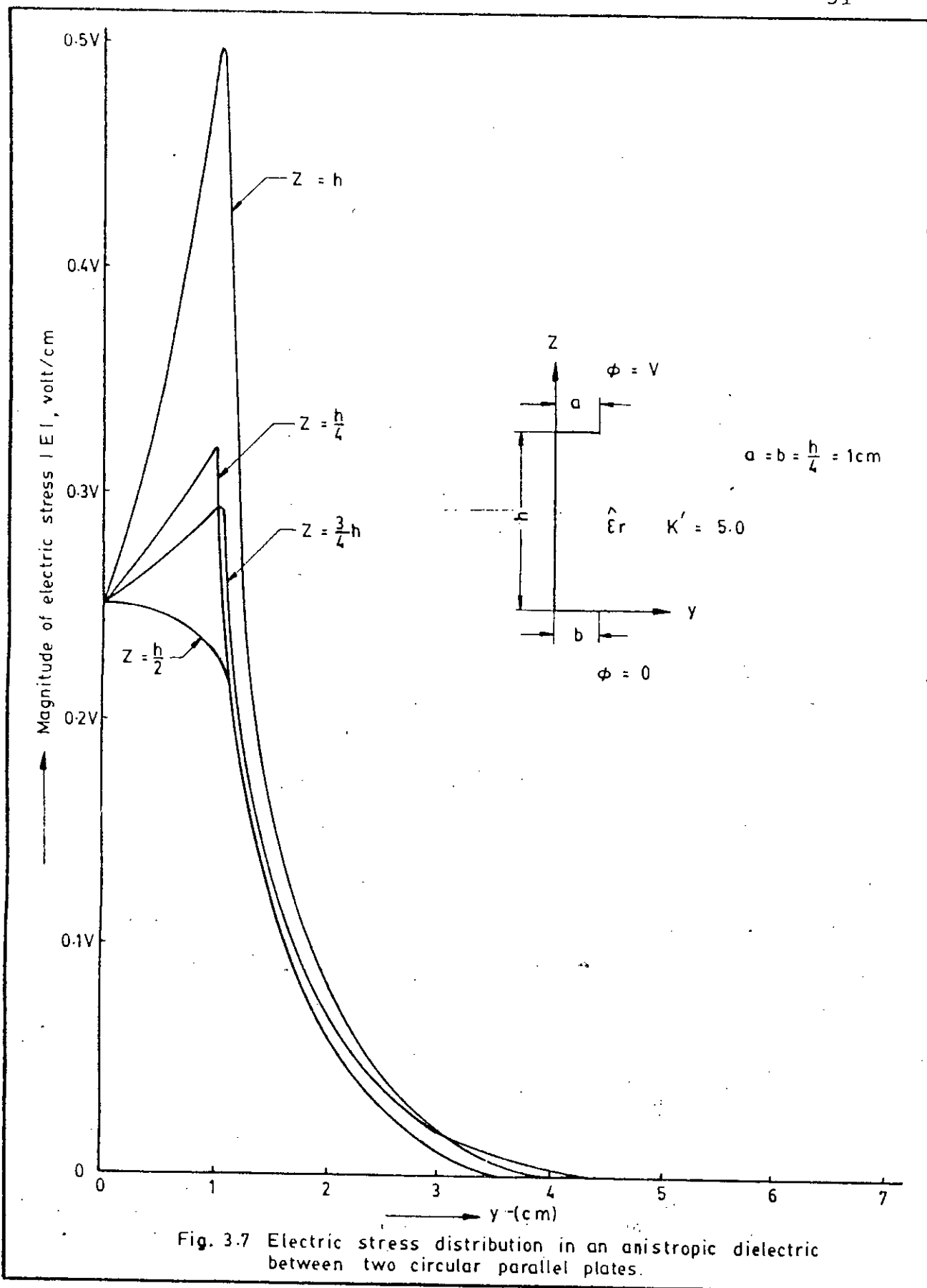


Fig. 3.7 Electric stress distribution in an anisotropic dielectric between two circular parallel plates.

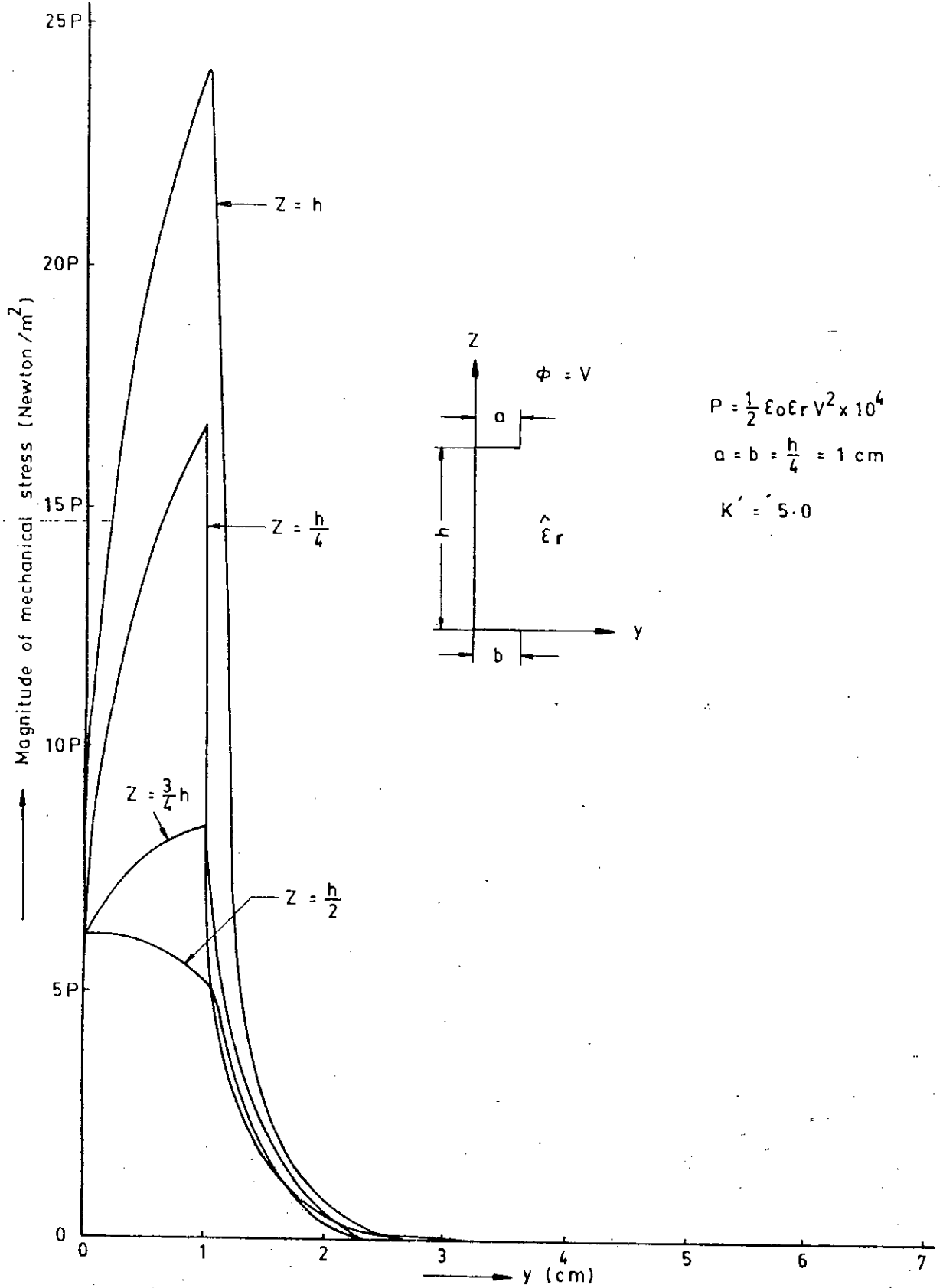


Fig.3.8. Mechanical stress distribution between two circular parallel plates at different heights in an anisotropic dielectric

Table 3.4: Variation of Mechanical and Electrical stress angle with the horizontal plane at different levels in an anisotropic dielectric between two parallel circular plates with  $k'=5.0$ ,  $a=b= h/2 = 2$  cm.

$z$ (cm) \ $y$ (cm)	0	1	2	3	4	5	6	7
4 $\theta_e$	$-90^\circ$	$-33.17^\circ$	$-24.42^\circ$	$-21.47^\circ$	$-20.73^\circ$	$-90^\circ$	$-90^\circ$	$-90^\circ$
$\theta_m$	$+90^\circ$	$-189.86^\circ$	$-180.39^\circ$	$-176.7^\circ$	$-175.72^\circ$	$+90^\circ$	$+90^\circ$	$+90^\circ$
3 $\theta_e$	$-86.93^\circ$	$-53.26^\circ$	$-52.10^\circ$	$-51.89^\circ$	$-51.96^\circ$	$-90^\circ$	$-90^\circ$	$-90^\circ$
$\theta_m$	$+96.13^\circ$	$-210.76^\circ$	$-209.44^\circ$	$-209.2^\circ$	$-209.28^\circ$	$+90^\circ$	$+90^\circ$	$+90^\circ$
2 $\theta_e$	$-90^\circ$	$-90^\circ$	$-90^\circ$	$-90^\circ$	$-90^\circ$	$-90^\circ$	$-90^\circ$	$-90^\circ$
$\theta_m$	$+90^\circ$	$+90^\circ$	$+90^\circ$	$+90^\circ$	$+90^\circ$	$+90^\circ$	$+90^\circ$	$+90^\circ$
1 $\theta_e$	$-93^\circ$	$-123.26^\circ$	$-144.07^\circ$	$-150.21^\circ$	$-151.86^\circ$	$-90^\circ$	$-90^\circ$	$-90^\circ$
$\theta_m$	$+84.01^\circ$	$+34.86^\circ$	$+12.64^\circ$	$+6.36^\circ$	$+4.6^\circ$	$+90^\circ$	$+90^\circ$	$+90^\circ$
0 $\theta_e$	$-90^\circ$	$-175.31^\circ$	$-175.44^\circ$	$-175.48^\circ$	$-175.48^\circ$	$-90^\circ$	$-90^\circ$	$-90^\circ$
$\theta_m$	$+90^\circ$	$-49.67^\circ$	$-50.52^\circ$	$-50.78^\circ$	$-50.78^\circ$	$+90^\circ$	$+90^\circ$	$+90^\circ$

Evidently in an anisotropic dielectric the field vector does not generally bisect the angle between the normal and the mechanical stress on a surface element. In special cases it happens so when  $\theta_e = 0^\circ$  and  $-90^\circ$ .

Fig. 3.7 and Fig. 3.8 indicates the electro-mechanical stress distribution in an anisotropic dielectric between two circular parallel plates. The corresponding stress angles are shown in Table 3.4. It is observed that the peak values of both electric and mechanical stresses rise with the development of anisotropy in the dielectric. But like the isotropic case, here the peak stress value occurs at the edge of the upper plate. As the distance increases from the edge of the parallel plates, the electromechanical stress die out more rapidly than the isotropic case. At the level  $z = \frac{h}{2}$  the electro-mechanical stresses are oppositely directed and have only normal components. Above and below this plane, both electric and mechanical stresses have lateral components. At the edge of the upper plate the mechanical stress is highly compressive. Tensile stresses are developed in the lower plate producing intensified shear stress in the plane  $z = \frac{h}{2}$ .

### 3.5 DISCUSSION

In this chapter, electromechanical stress distributions in both isotropic and anisotropic dielectrics between two

circular parallel plates have been studied. In section 3.2, generalized equation for the calculation of electromechanical stresses for both free space and dielectric media has been developed. In section 3.3, the electromechanical stress distributions have been calculated between two circular parallel plates in an isotropic dielectric. Both magnitudes and angles of stress values at different points are calculated. Peak value of stresses occur at the edge of the upper plate and is independent of the size of the plates. It is also observed that for isotropic dielectric, the electric stress bisects the angle between the normal  $\bar{n}$  and the mechanical stress. At the edge of the plates lateral stresses become dominant and the stress is almost normal at the mid-level. The high lateral stress at the upper and lower plates may cause dielectric breakdown. With the increase of anisotropy in the medium, peak value of both the electric and mechanical stresses rises and also the lateral component of stress increases. Again, it is observed that beyond the plates, the stresses die out more rapidly in the anisotropic case compared to the isotropic case. But like the isotropic media, here the electric stress does not always bisect the angle between the normal and the mechanical stress.



## CHAPTER 4

## ELECTROMECHANICAL STRESS DISTRIBUTION IN FERROELECTRIC INSULATORS.

4.1 INTRODUCTION:

In dielectric materials discussed so far, the polarization is a linear function of the applied field. There are, however, a number of substances for which the polarization of a specimen is not a linear function of the field strength. These materials exhibit hysteresis effects like the ferromagnetic materials. These are called ferroelectric materials. Electromechanical stress analysis in such media has not yet been reported.

An applied electric field induces dipole moments in atoms or ions, and generally displaces ions relative to each other. Consequently, the dimensions of a specimen undergo slight changes. So, in most materials dielectric polarization produces a mechanical distortion, but a mechanical distortion does not produce polarization. This electromechanical effect, which is present in all materials, is called electrostriction. There are various types of ferroelectric materials that are used in high voltage insulators because of their very high relative permittivity.

#### 4.2 REVIEW OF THE PROPERTIES OF FERROELECTRIC MATERIALS:

Barium titanate (BT) materials are commonly used in the fabrication of capacitors (insulators) with a multilayered structure. This is a very important ferroelectric material for the high voltage insulator. Their high permittivity enables fabrication of capacitors which have high capacitance but are small in size. There are three types of BT materials commonly used in insulators. These are: NPO ( $\epsilon_r \sim 60$ ), x7R ( $\epsilon_r \sim 1800$ ) and Z5u ( $\epsilon_r \sim 9000$ ). As discussed in section 4.1, hysteresis effects are present in ferroelectric materials.

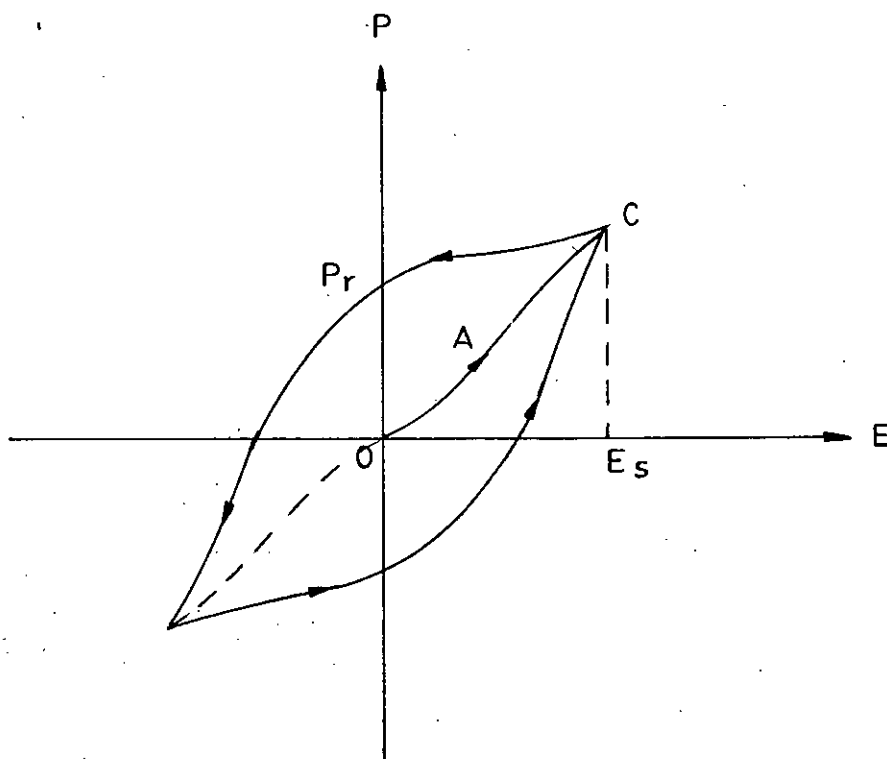


Fig.4.1 The hysteresis curve of ferroelectric material

When an electric field is applied to a virgin specimen, the polarization increases along the curve OAC as shown in Fig. 4.1. If the field is reduced to zero, it is found that for  $E=0$ , a certain amount of polarization  $p_r$  remains known as remanant polarization. Thus the material is spontaneously polarized. For polarization experiencing hysteresis curve the magnitude of the electric flux density as a function of the electric field can be well approximated as

$$D = \epsilon_0 (\epsilon_{r0} E - kE^3) \quad \dots \quad (4.1)$$

where  $\epsilon_0 \epsilon_{r0} = \left. \frac{dD}{dE} \right|_{E=0}$

$\epsilon_{r0}$  is therefore the dielectric constant at very weak field.  $K$  is a constant. Again we have

$$D = \epsilon_0 E + P \quad \dots \quad (4.2)$$

where  $P$  accounts for the amount of polarization. Equating (4.1) and (4.2) we get

$$P = \epsilon_0 \left[ (\epsilon_{r0} - 1) E - kE^3 \right] \quad \dots \quad (4.3)$$

The effective relative permittivity  $\epsilon_r$  is obtained from

$$\epsilon_0 (\epsilon_r - 1) = \frac{dP}{dE} \quad \dots \quad (4.4)$$

Substituting (4.3) into (4.4)

$$\epsilon_0 (\epsilon_r - 1) = \epsilon_0 \left[ (\epsilon_{r0} - 1) - 3kE^2 \right]$$

$$\text{or } \epsilon_r = \epsilon_{r0} - 3kE^2 \quad \dots \quad (4.5)$$

Saturated polarization takes place when  $E=E_s$

where  $\frac{dP}{dE} = 0$ , so that at saturation  $\epsilon_r = 1$ . Hence by (4.5) the constant  $k$  is determined as

$$k = \frac{\epsilon_{r0} - 1}{3E_s^2} \quad \dots \quad (4.6)$$

The relative permittivity versus the applied field strength takes the form shown in fig. (4.2).

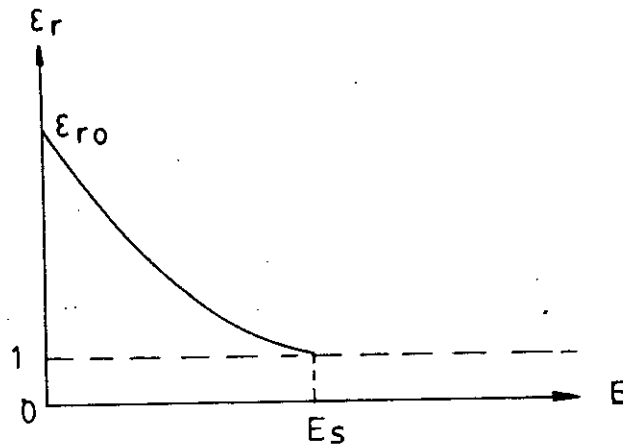


Fig.4.2 Variation of relative permittivity with the applied field

After saturation the field leaks out into the medium surrounding the ferroelectric material. From equation (4.5) it is evident that as the field strength increases the relative permittivity of the material decreases causing leakage of flux outside the ferroelectric material. The ferroelectric material behaves as a non-linear medium. Flash-over around insulators takes place with the air breakdown at which the field strength is  $15 \times 10^5$  v/m. We choose  $E_s = \frac{2}{3} \times 15 \times 10^5$  v/m.  $= 10^6$  v/m.  $\epsilon_{ro} = 2,000$  for ceramic.

Laplace's equation in a charge-free region is given in rectangular co-ordinates as

$$\frac{\partial D_x}{\partial x} + \frac{\partial D_y}{\partial y} + \frac{\partial D_z}{\partial z} = 0 \quad \dots \quad (4.7)$$

From eqn. (4.1) for ferroelectric materials

$$D_x = \epsilon_o (\epsilon_{ro} E_x - k E_x^3) \quad \dots \quad (4.8)$$

$$D_y = \epsilon_o (\epsilon_{ro} E_y - k E_y^3) \quad \dots \quad (4.9)$$

$$D_z = \epsilon_o (\epsilon_{ro} E_z - k E_z^3) \quad \dots \quad (4.10)$$

Substituting (4.8) - (4.10) into (4.7).

$$\epsilon_{ro} \left( \frac{\partial E_x}{\partial x} + \frac{\partial E_y}{\partial y} + \frac{\partial E_z}{\partial z} \right) - 3k \left( E_x^2 \frac{\partial E_x}{\partial x} + E_y^2 \frac{\partial E_y}{\partial y} + E_z^2 \frac{\partial E_z}{\partial z} \right) = 0$$

$$\text{or } (\epsilon_{ro} - 3kE_x^2) \frac{\partial E_x}{\partial x} + (\epsilon_{ro} - 3kE_y^2) \frac{\partial E_y}{\partial y} + (\epsilon_{ro} - 3kE_z^2) \frac{\partial E_z}{\partial z} = 0$$

$$\epsilon_{ro} \left( \frac{\partial^2 \phi}{\partial x^2} + \frac{\partial^2 \phi}{\partial y^2} + \frac{\partial^2 \phi}{\partial z^2} \right) - 3k \left[ \left( \frac{\partial \phi}{\partial x} \right)^2 \frac{\partial^2 \phi}{\partial x^2} + \left( \frac{\partial \phi}{\partial y} \right)^2 \frac{\partial^2 \phi}{\partial y^2} + \left( \frac{\partial \phi}{\partial z} \right)^2 \frac{\partial^2 \phi}{\partial z^2} \right] = 0 \quad (4.11)$$

Now if finite element method is applied the potential function  $\phi$  with piecewise linearization on each triangular element satisfies the above equation.

#### 4.3 ELECTROMECHANICAL STRESS ANALYSIS IN FERROELECTRIC INSULATORS

Ferroelectric materials undergo non-linear polarization. Moreover with the application of an A.C. field these materials undergo hysteresis effects arising from remanent polarization. For D.C. fields the electric flux density can be given by

$$D_x = \epsilon_0 (\epsilon_{ro} E_x - kE_x^3) \quad \dots \quad (4.12)$$

$$D_y = \epsilon_0 (\epsilon_{ro} E_y - kE_y^3) \quad \dots \quad (4.13)$$

$$D_z = \epsilon_0 (\epsilon_{ro} E_z - kE_z^3) \quad \dots \quad (4.14)$$

With  $\bar{E} = -\nabla\phi$  let us consider the identity

$$(\nabla \times \bar{E}) \times \bar{D} = \begin{vmatrix} \bar{i} & \bar{j} & \bar{k} \\ \frac{\partial E_z}{\partial y} - \frac{\partial E_y}{\partial z} & \frac{\partial E_x}{\partial z} - \frac{\partial E_z}{\partial x} & \frac{\partial E_y}{\partial x} - \frac{\partial E_x}{\partial y} \\ D_x & D_y & D_z \end{vmatrix} \quad \dots \quad (4.16)$$

In the above the x, y and z components of the vector are given by

$$\left[ (\nabla \times \bar{E}) \times \bar{D} \right] \cdot \bar{i} = D_z \left( \frac{\partial E_x}{\partial z} - \frac{\partial E_z}{\partial x} \right) - D_y \left( \frac{\partial E_y}{\partial x} - \frac{\partial E_x}{\partial y} \right) = 0 \quad \dots \quad (4.17)$$

$$\left[ (\nabla \times \bar{E}) \times \bar{D} \right] \cdot \bar{j} = D_x \left( \frac{\partial E_y}{\partial x} - \frac{\partial E_x}{\partial y} \right) - D_z \left( \frac{\partial E_x}{\partial x} - \frac{\partial E_y}{\partial z} \right) = 0 \quad \dots \quad (4.18)$$

$$\left[ (\nabla \times \bar{E}) \times \bar{D} \right] \cdot \bar{k} = D_y \left( \frac{\partial E_x}{\partial x} - \frac{\partial E_y}{\partial z} \right) - D_x \left( \frac{\partial E_x}{\partial z} - \frac{\partial E_z}{\partial x} \right) = 0 \quad \dots \quad (4.19)$$

The above equations can be arranged by adding equal quantities on both sides such as

$$D_z \left( \frac{\partial E_x}{\partial z} - \frac{\partial E_z}{\partial x} \right) - D_y \left( \frac{\partial E_y}{\partial x} - \frac{\partial E_x}{\partial y} \right) + E_x \nabla \cdot \bar{D} = E_x \nabla \cdot \bar{D}$$

... (4.20)

$$D_x \left( \frac{\partial E_y}{\partial x} - \frac{\partial E_x}{\partial y} \right) - D_z \left( \frac{\partial E_x}{\partial x} - \frac{\partial E_y}{\partial z} \right) + E_y \nabla \cdot \bar{D} = E_y \nabla \cdot \bar{D}$$

... (4.21)

$$D_y \left( \frac{\partial E_z}{\partial y} - \frac{\partial E_y}{\partial z} \right) - D_x \left( \frac{\partial E_x}{\partial z} - \frac{\partial E_z}{\partial x} \right) + E_z \nabla \cdot \bar{D} = E_z \nabla \cdot \bar{D}$$

... (4.22)

The above three equations can be arranged in tensor form

$$\nabla \cdot \hat{S} \bar{I} = \bar{E} \nabla \cdot \bar{D}$$

... (4.23)

where  $\hat{S}$  is the stress tensor

$$\hat{S} = \begin{bmatrix} S_{11} & S_{12} & S_{13} \\ S_{21} & S_{22} & S_{23} \\ S_{31} & S_{32} & S_{33} \end{bmatrix}$$

... (4.24)

67816



$\bar{I}$  is the column vector

$$\bar{I} = \begin{bmatrix} \bar{i} \\ \bar{j} \\ \bar{k} \end{bmatrix} \quad \dots \quad (4.25)$$

The elements  $S_{ij}$  of the tensor elements are given by

$$S_{11} = \epsilon_0 \left[ \epsilon_{ro} (E_x^2 - \frac{1}{2} E^2) + \frac{k}{4} (E_y^4 + E_z^4 - 3E_x^4) \right] \quad \dots \quad (4.26)$$

$$S_{12} = \epsilon_0 ( \epsilon_{ro} E_y - kE_y^3 ) E_x \quad \dots \quad (4.27)$$

$$S_{13} = \epsilon_0 ( \epsilon_{ro} E_z - kE_z^3 ) E_x \quad \dots \quad (4.28)$$

$$S_{21} = \epsilon_0 ( \epsilon_{ro} E_x - kE_x^3 ) E_y \quad \dots \quad (4.29)$$

$$S_{22} = \epsilon_0 \left[ \epsilon_{ro} (E_y^2 - \frac{1}{2} E^2) + \frac{k}{4} (E_z^4 + E_x^4 - 3E_y^4) \right] \quad \dots \quad (4.30)$$

$$S_{23} = \epsilon_0 ( \epsilon_{ro} E_z - kE_z^3 ) E_y \quad \dots \quad (4.31)$$

$$S_{31} = \epsilon_0 ( \epsilon_{ro} E_x - kE_x^3 ) E_z \quad \dots \quad (4.32)$$

$$S_{32} = \epsilon_0 ( \epsilon_{ro} E_y - kE_y^3 ) E_z \quad \dots \quad (4.33)$$

$$S_{33} = \epsilon_0 \left[ \epsilon_{ro} (E_z^2 - \frac{1}{2} E^2) + \frac{k}{4} (E_x^4 + E_y^4 - 3E_z^4) \right] \quad \dots \quad (4.34)$$

Derivation of the stress element  $S_{ij}$  is given in the appendix A.2.

$$\text{where } E = \sqrt{E_x^2 + E_y^2 + E_z^2}$$

The resulting electromechanical force equation is given by taking volume integral over (4.23).

$$\int_V \nabla \cdot \hat{S} \bar{I} \, dv = \int_V \bar{E} \nabla \cdot \bar{D} \, dv \quad \dots \quad (4.35)$$

$$\text{or } \oint_a \hat{S} \bar{I} \cdot \bar{n} \, da = \int_V \bar{E} \nabla \cdot \bar{D} \, dv \quad \dots \quad (4.36)$$

$$\text{using } \bar{D} = \bar{D}_o + \bar{P} \text{ and } \nabla \cdot \bar{D}_o = \rho$$

$$\oint_a \hat{S} \bar{I} \cdot \bar{n} \, da = \int_V \bar{E} \rho \, dv \text{ on the charged regions.}$$

$$\oint_a \hat{S} \bar{I} \cdot \bar{n} \, da = \int_V \bar{E} \nabla \cdot \bar{P} \, dv. \text{ in the insulator.}$$

#### 4.4 ELECTROMECHANICAL STRESS DISTRIBUTION IN A FERROELECTRIC INSULATOR BETWEEN TWO CIRCULAR PARALLEL PLATES

For a linear medium we have flux density

$$D_{x0} = \epsilon_o \epsilon_{r0} E_{x0}$$

$$\text{and } D_{y0} = \epsilon_o \epsilon_{r0} E_{y0}$$

where ,  $\epsilon_{ro}$  is the dielectric constant for a very weak field in ferroelectric material;  $E_{x0}$ ,  $E_{y0}$  are the field components for linear polarization. These field components can be readily determined by finite element method.

Let the corresponding fields be  $E_x$  and  $E_y$  which will maintain the same flux density in ferroelectric material exhibiting non-linear polarization.

So, we get,

$$D_x = \epsilon_{ro} E_x - kE_x^3 = \epsilon_{ro} E_{x0} \quad \dots \quad (4.37)$$

$$D_y = \epsilon_{ro} E_y - kE_y^3 = \epsilon_{ro} E_{y0} \quad \dots \quad (4.38)$$

Solving these cubic eqns. for  $E_x$  and  $E_y$  in terms of  $E_{x0}$  and  $E_{y0}$ . We will get the electric fields in ferroelectric materials. The method of obtaining the nonlinear solution from the linear one as discussed above can be graphically explained with the aid of Fig. 4.3.

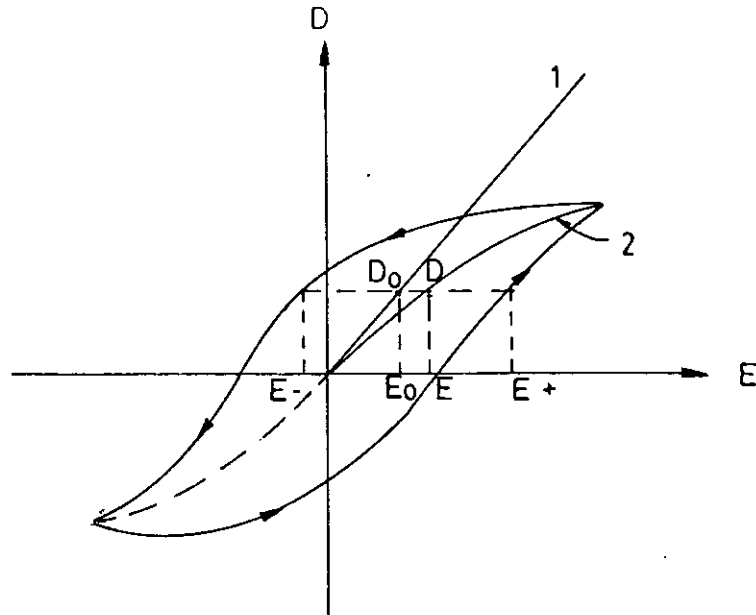


Fig.4.3 Graphical method of obtaining non-linear field solution from the linear solution

The linear variation of  $D$  with  $E$  is represented by the straight line 1. The non-linear variation is represented by the curve 2. Now for constant flux density,  $D = D_0$  so that  $E$  can be readily obtained from  $E_0$ . Similarly considering the hysteresis effects for alternating fields,  $E+$  and  $E-$  can be graphically determined. If we take the case of two circular parallel plates symmetrical about the  $y$ -axis, then in eqn. (4.36).

$$n_x = 0, n_z = 0 \text{ and } n_y = 1$$

and  $E_z = 0$

So, the  $x$  component of the mechanical stress will be  $t_x = S_{12}$  and the  $y$  component of the mechanical stress will be  $t_y = S_{22}$ . Hence from equation (4.15) and (4.18) we get

$$t_x = S_{12} = \epsilon_0 (\epsilon_{ro} - kE_y^2) E_x E_y \quad \dots \quad (4.39)$$

$$t_y = S_{22} = \epsilon_0 \left[ \frac{\epsilon_{ro}}{2} ( E_y^2 - E_x^2 ) + \frac{k}{4} ( E_x^4 - 3E_y^4 ) \right] \dots (4.40)$$

The resultant mechanical stress is given by

$$t = \sqrt{t_x^2 + t_y^2} \dots (4.41)$$

It can be readily checked that  $t \neq \frac{1}{2} \bar{D} \cdot \bar{E}$  for a non-linear medium.

For alternating fields experiencing hysteresis effects the electric field components in the above expression must be changed as  $E \pm E_s/2$  respectively for alternation from negative maximum to positive maximum and positive maximum to negative maximum. Here  $E_s/2$  represents the assumed magnitude of the field strength with the remanant polarization.

Both electric and mechanical stress has been calculated in ferroelectric insulator between two parallel plates. If an electrostatic potential is applied, then it is found that maximum electric stress occurs at the edge of the upper plate at  $y = h$ . As the distance from the edge of the plate increases, the electric stress drops off rapidly. Again the stress at the lower plate i.e. at  $y = 0$  is higher than at a level between the plates. The stress at  $y = \frac{h}{4}$  becomes

maximum on the edge of the lower plate. These are shown in figs. ( 4.4-5 ) . If the field is alternating, then some different nature of the stress curve is observed. In the cycle when the applied voltage alternates from +ve max<sup>m</sup> to -ve maximum, then the stress distribution takes the forms shown figs. 4.6-7. The corresponding variation of stress angles is shown in table 4.2. Like the electrostatic case, here also the maximum stress occurs at the edge (i.e.  $x=a$ ). The lower plate here attains minimum stress level. As the distance increases, the stress curves converges to a constant value which is attributed to the remanent polarization. Here the peak stress value is larger than the electrostatic case. But for the case when the applied potential alternates from +ve maximum to +ve then a different type of stress variation takes place as shown in figs. 4.8-9 with the angle variation shown table 4.3. Unlike the previous cases the peak stress here occurs at the edges of lower plate and the upper plate is at minimum stress. The stress curves attain constant stress value as the distance  $x$  increases. Compared to the former two cases, it is evident that the peak stress value is maximum for the present case. So, for alternating voltages, the insulator should be so designed as to withstand the peak stress at the two plates in the form of compression or tension.

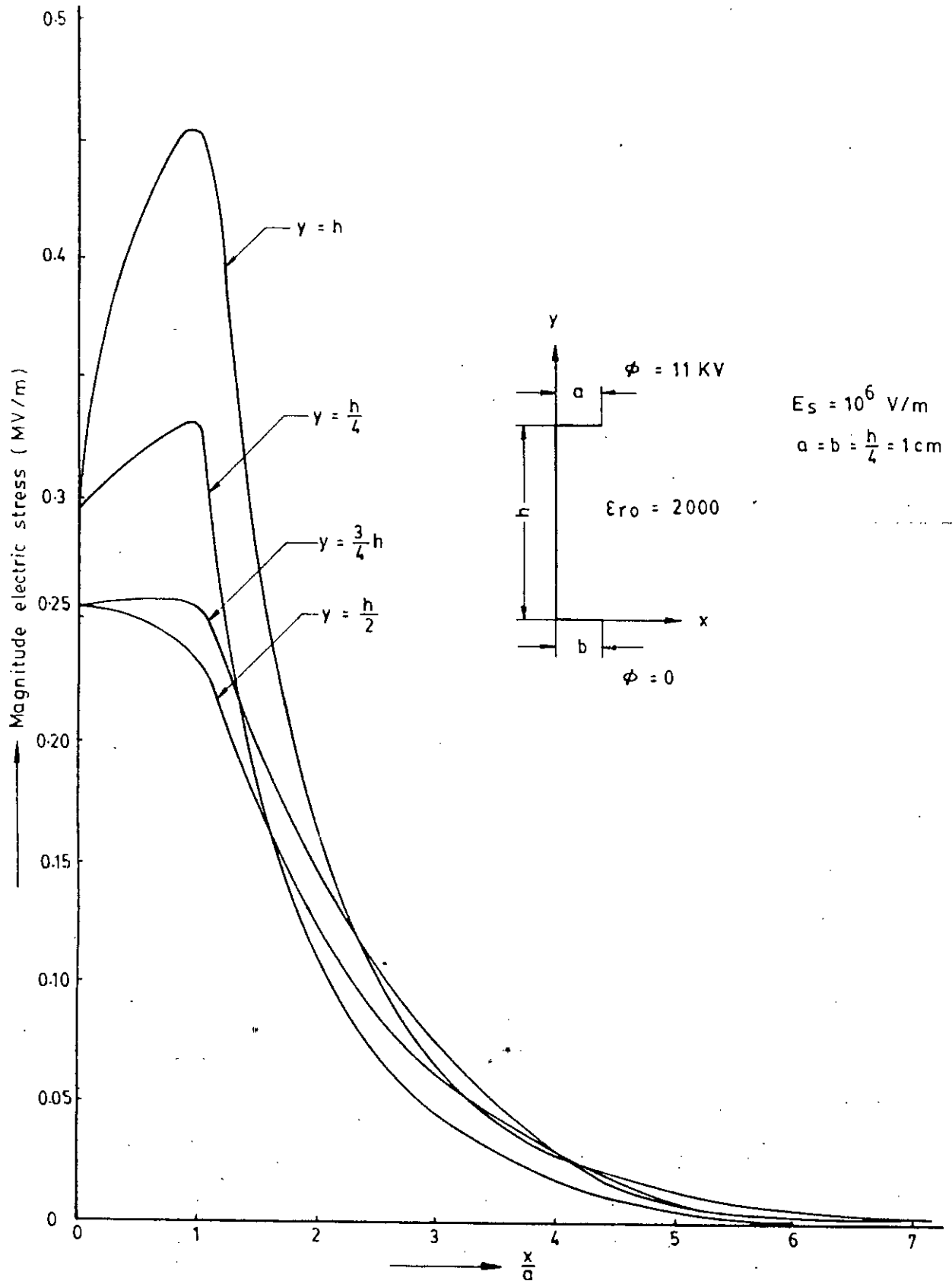


Fig.4.4. Electric stress distribution in ferroelectric insulators at different heights under static case

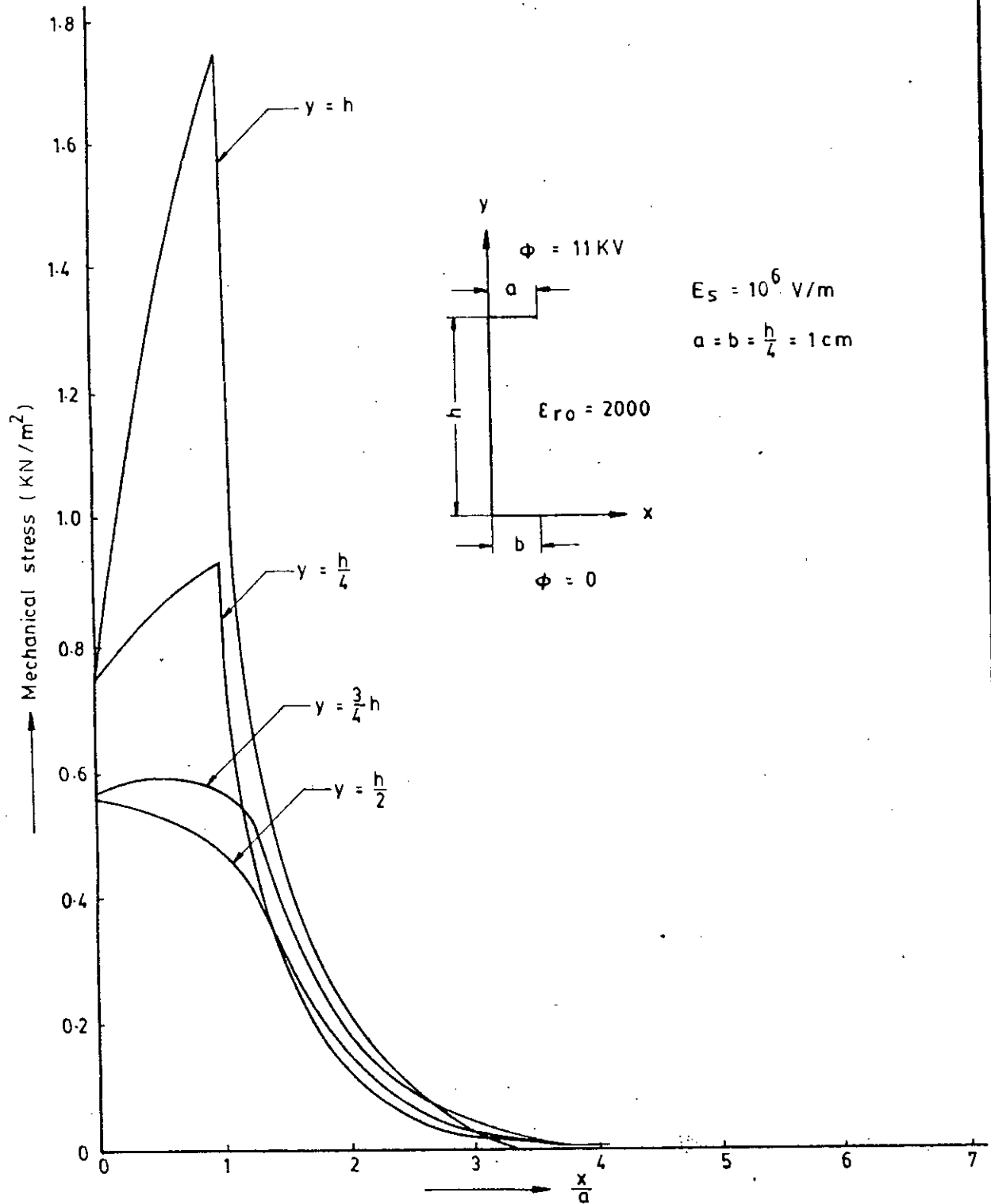


Fig. 4.5. Mechanical stress distribution in ferroelectric insulator at different heights (static case)



Table 4.1: Variation of Electrical and Mechanical angles at different points between two parallel plates in Ferroelectric media.  
(For static case)  $\epsilon_{ro} = 2000.0$

$x$ (cm) $y$ (cm)	0	1	2	3	4	5	6	7	
	$\theta_e$ $\theta_m$								
4	$\theta_e$ $\theta_m$	$-90.05^\circ$ $+89.96^\circ$	$-44.59^\circ$ $-178.18^\circ$	$-37.33^\circ$ $-164.57^\circ$	$-32.96^\circ$ $-155.87^\circ$	$-30.93^\circ$ $-151.82^\circ$	$-30.64^\circ$ $-151.24^\circ$	$-33.45^\circ$ $-156.86^\circ$	$-52.37^\circ$ $-194.7^\circ$
3	$\theta_e$ $\theta_m$	$-85.51^\circ$ $-260.88^\circ$	$-66.68^\circ$ $-222.87^\circ$	$-63.80^\circ$ $-217.4^\circ$	$-62.87^\circ$ $-215.65^\circ$	$-62.66^\circ$ $-215.26^\circ$	$-63.17^\circ$ $-216.29^\circ$	$-65.92^\circ$ $-221.8^\circ$	$-77.27^\circ$ $-244.5^\circ$
2	$\theta_e$ $\theta_m$	$-90.04^\circ$ $+90.04^\circ$	$-90.04^\circ$ $+90.04^\circ$	$-90.04^\circ$ $+90.04^\circ$	$-90.04^\circ$ $+90.04^\circ$	$-90.04^\circ$ $+90.04^\circ$	$-90.04^\circ$ $+90.04^\circ$	$-90.03^\circ$ $+90.04^\circ$	$-90.03^\circ$ $+90.04^\circ$
1	$\theta_e$ $\theta_m$	$-93.87^\circ$ $82.09^\circ$	$-107.77^\circ$ $53.78^\circ$	$-124.08^\circ$ $21.70^\circ$	$-133.88^\circ$ $2.19^\circ$	$-138.28^\circ$ $-6.60^\circ$	$-139.45^\circ$ $-8.94^\circ$	$-136.68^\circ$ $-3.40^\circ$	$-118.48^\circ$ $+32.99^\circ$
0	$\theta_e$ $\theta_m$	$-90.05^\circ$ $+90.04^\circ$	$-163.22^\circ$ $-56.07^\circ$	$-164.3^\circ$ $-58.59^\circ$	$164.76^\circ$ $-59.55^\circ$	$164.82^\circ$ $-59.69^\circ$	$-164.10^\circ$ $-58.25^\circ$	$-160.13^\circ$ $-50.32^\circ$	$-134.99^\circ$ $-0.02^\circ$

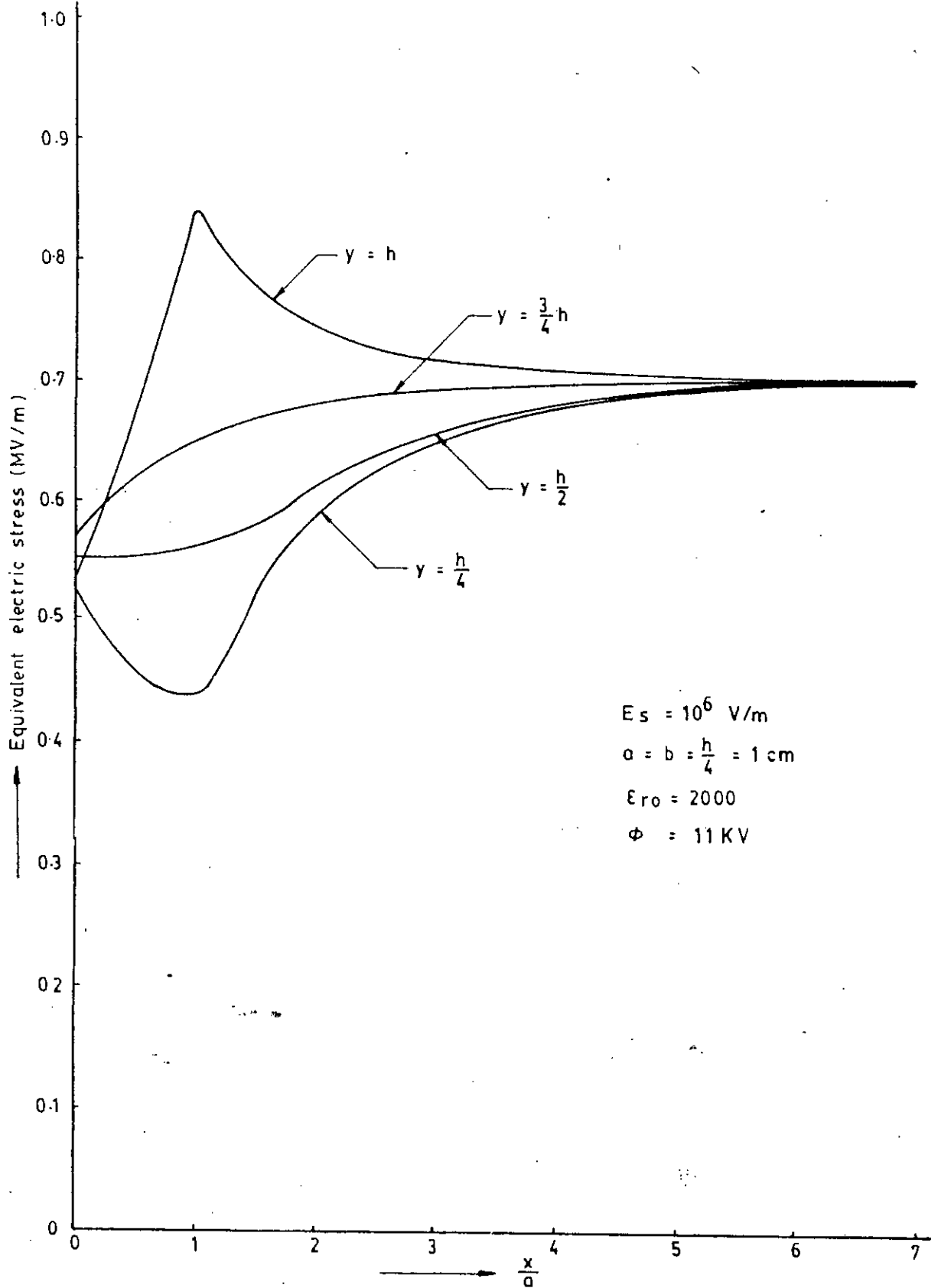


Fig. 4.6. Electric stress variation in ferroelectric insulators when the applied voltage alternates from +ve maximum to -ve max.



Table 4.2: Distribution of mechanical and electrical stress angles at different points when the applied potential alternates  $E_s = 10^6$  v/m from +ve maximum to -ve maximum

$x$ (cm) \ $y$ (cm)	0	1	2	3	4	5	6	7
4 $\theta_e$	21.10	12.52	32.72	39.92	42.75	43.98	44.55	44.84
$\theta_m$	-44.91	-62.40	-24.59	-11.83	-6.75	-4.51	-3.46	-2.93
3 $\theta_e$	25.09	23.68	32.95	39.02	42.14	43.65	44.38	44.72
$\theta_m$	-38.99	-41.39	-24.18	-13.27	-7.72	-5.03	-3.75	-3.13
2 $\theta_e$	25.98	27.83	36.26	40.90	43.09	44.11	44.57	44.78
$\theta_m$	-37.35	-33.80	-18.09	-9.76	-5.93	-4.17	-3.37	-3.03
1 $\theta_e$	22.94	24.65	42.88	44.94	45.13	45.09	45.03	44.98
$\theta_m$	-43.33	-40.23	-5.78	-2.38	-2.23	-2.40	-2.54	-2.67
0 $\theta_e$	20.07	66.22	51.28	47.50	46.11	45.50	45.21	45.02
$\theta_m$	-48.91	41.00	10.02	2.34	-0.45	-1.65	-2.24	-2.59

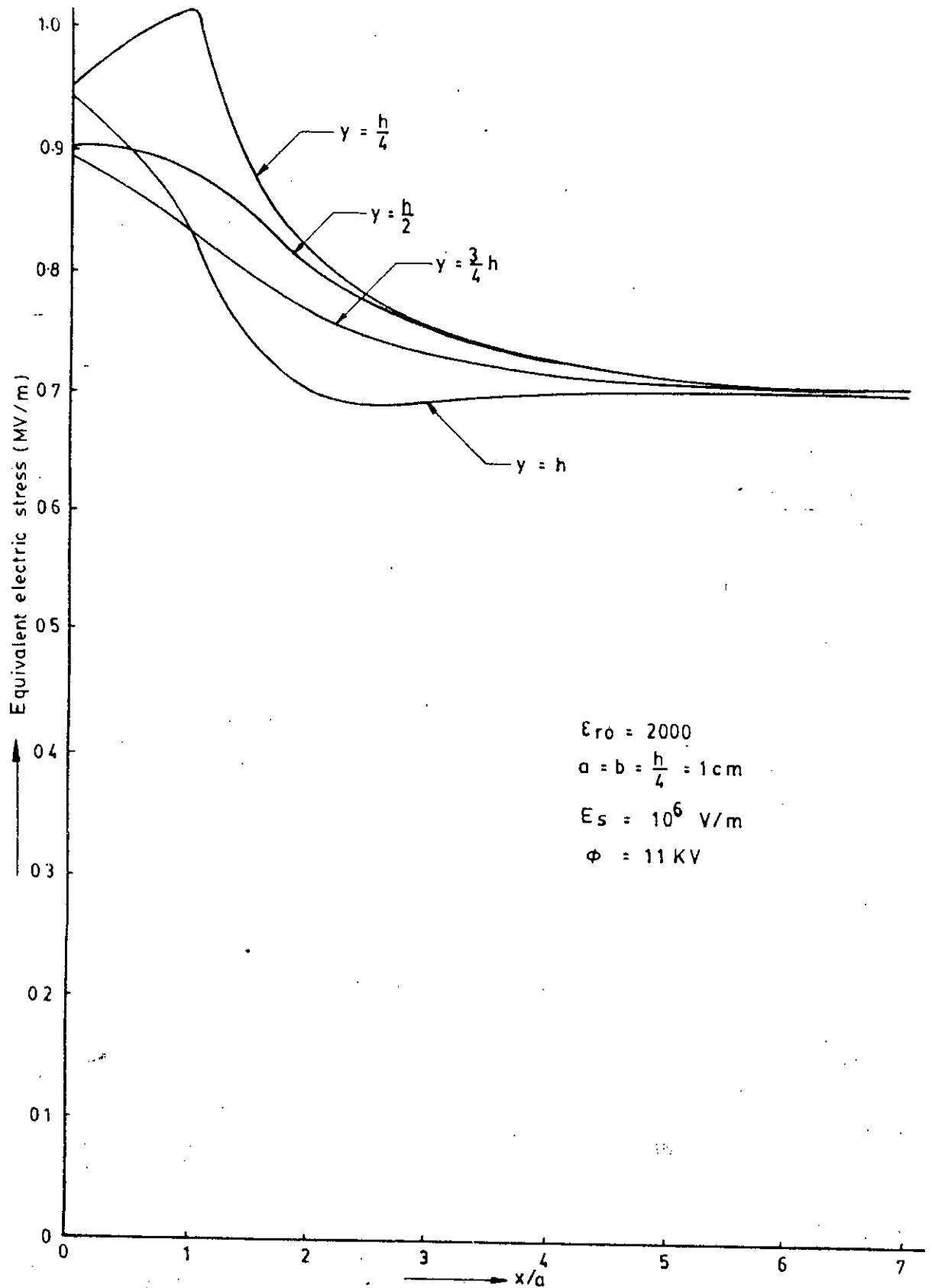


Fig. 4.8. Electric stress distribution in ferroelectric insulator at different heights, when the applied voltage alternates from -ve maximum to +ve maximum

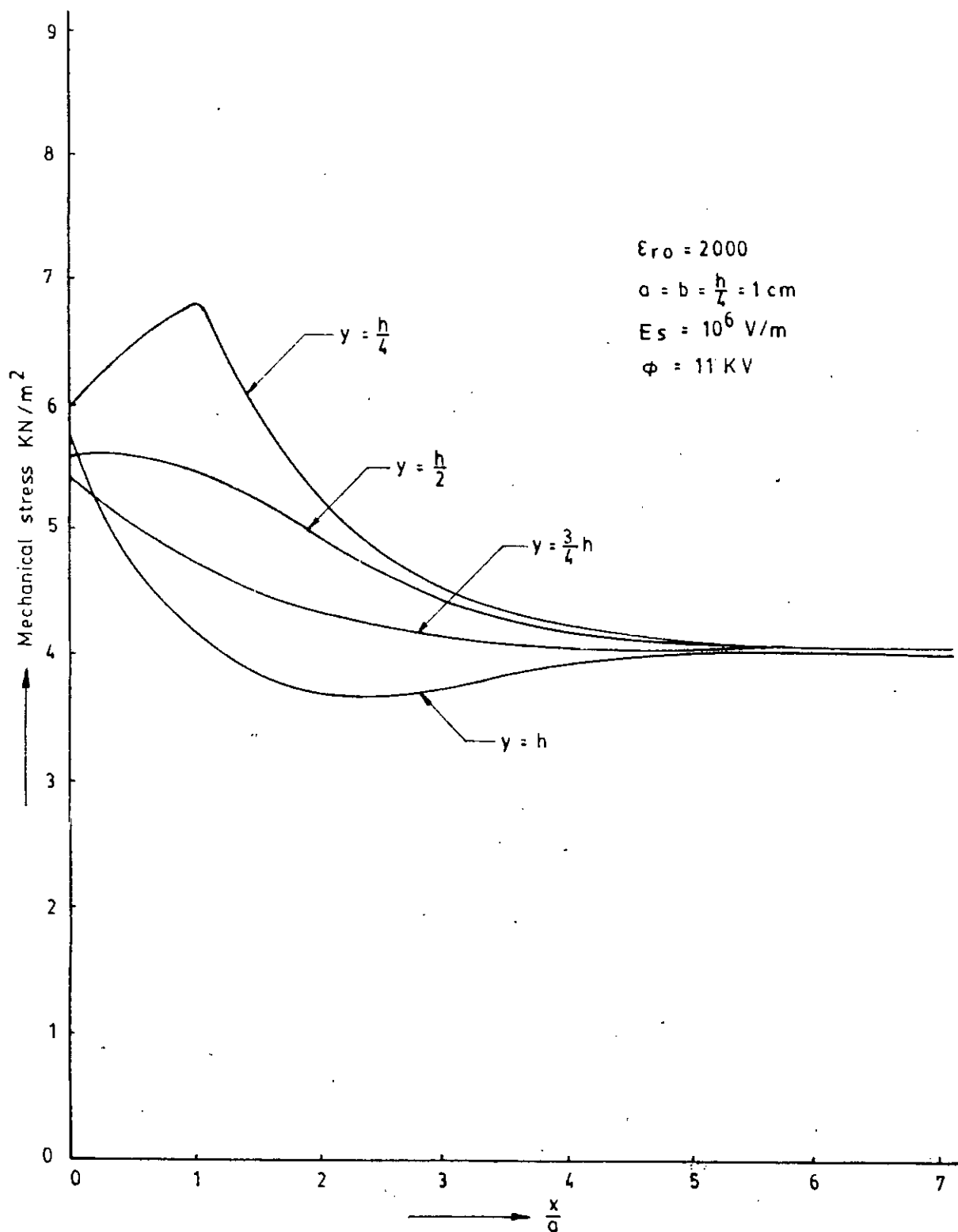


Fig.4.9. Mechanical stress distribution in ferroelectric insulator when the applied voltage alternates from -ve maximum to +ve maximum.

Table 4.3: Angle of Electrical and mechanical stress distribution  
 (Ferro electric material) Applied potential goes from -ve maximum  
 to +ve maximum.

$\epsilon_{r0} = 2000$        $a=b= \frac{h}{4} = 1 \text{ cm.}$        $E_s = 10^6 \text{ v/m.}$

y \ x	0	1	2	3	4	5	6	7
	$\theta_e$ $\theta_m$							
4	-122.07 17.16	-102.23 61.38	-121.93 21.89	-129.67 7.22	-132.65 1.68	-133.92 -0.67	-134.5 -1.74	-134.8 -2.28
3	-122.35 17.69	-118.37 26.65	-124.4 16.18	-129.36 7.38	-132.19 2.35	-133.63 -0.21	-134.34 -1.47	-134.68 -2.08
2	-123.43 15.44	-124.16 14.46	-128.26 8.42	-131.38 3.43	-133.17 0.46	-134.09 -1.09	-134.54 -1.85	-134.73 -2.19
1	-123.11 14.99	-126.34 7.78	-133.43 -0.97	-134.91 -2.89	-135.08 -2.97	-135.04 -2.81	-134.99 -2.66	-134.93 -2.54
0	-121.42 17.92	-144 -19.54	-139.48 -11.35	-137.13 -6.82	-135.99 -4.61	-135.44 -3.52	-135.16 -2.97	-134.98 -2.62

#### 4.5 DISCUSSION

In the above, electromechanical stress distributions in ferroelectric insulators have been studied. Section 4.3 gives the general form of stress analysis in ferroelectric insulators. In section 4.4, electromechanical stress has been calculated and investigated between two parallel plates. First of all, we have taken the case of electrostatic voltage applied to the plates. For this case, the electromechanical stress distributions are given in Figs. 4.3-4. Corresponding angle variations are shown in table 4.1. Peak stress value has been found to occur at the edge of the top plate. Since the medium is non-linear here, to maintain the same flux density the electric fields are higher in this case. Angle variation is almost same as the isotropic case. At  $y = \frac{h}{2}$  the electromechanical stresses have only normal components and they are equal and opposite. But at the edge of top and bottom plates, the angle variations is such that they give rise to lateral components of stress.

As the applied potential alternates from +ve maximum to -ve maximum, some changes of stress distributions are observed as shown in Figs. 4.6-7. In this case, the maximum stress develops at the edge of upper plate and electromechanical stresses are higher than the static field case.



At the edges of upper and lower plates the angle variation is such that the dielectric between the plates undergo compressive stress. This angle variation is shown in Table 4.2. For the case when the applied potential alternates from -ve maximum to +ve maximum, the type of electromechanical stress distribution is shown in Figs. 4.8 and 4.9. The corresponding angle variations are shown in Table 4.3. The peak value of both electrical and mechanical stresses are higher than the above two cases but it occurs at the lower plate. Here the mechanical stress angles are such that the dielectric is subjected to tension. Thus as the applied potential alternates, the ferroelectric material within the two parallel plates is subjected to alternate compression and tension. In both the cases high lateral stresses are developed in the radially outward direction.

## CHAPTER 5

### GENERAL DISCUSSION AND CONCLUSION

A computer program has been developed for calculating the electromechanical stress distribution in insulators by finite element method. It involves rapid calculation of potential at different nodes, the electrical and mechanical stresses over different elements for both linear and non linear media.

To get an idea about the electro-mechanical stress over a region, it is first necessary to know the potential distribution over the region. The space between two circular parallel plates has been divided into a finite number of triangular elements. Then assuming linear dependence of potential over the elements, Laplace's equation has been solved to get the potential at different nodes. It is observed that in an isotropic dielectric between two circular parallel plates, the potentials at different nodes converge to the potential at the mid level between the parallel plates as the distance from the axis of the parallel plates increases. The above convergence of potentials becomes faster with the development of anisotropy in the dielectric. Potential distributions have been shown in Fig. 2.2 and Fig. 2.3 for the above two media.

Chapter 3 discusses the electromechanical stress analysis for both isotropic and anisotropic dielectrics between two circular parallel plates. In an isotropic dielectric the magnitudes of electromechanical stresses are plotted in Figs. 3.3 and 3.4 and corresponding stress angles are given in Table 3.2. For anisotropic case, the above results are shown in Figs. 3.7 and 3.8 and Table 3.4 respectively. It is understood from these plots that the peak value of electromechanical stress always occurs at the edge of the upper plate and the peak value rises with the increase of axial anisotropy in the dielectric. In the anisotropic case, the stress value dies out more rapidly as the distance from the axis of the plates increases. At the mid-level stresses are purely vertical but the lateral stresses in the upper and lower portions are oppositely directed giving rise to shear. For anisotropic case, this shear is intensified.

Since ferroelectric materials are extensively used in fabrication of high voltage insulators because of their high relative permittivity, a study has been given to the electromechanical stress distribution in such materials. Because of the nonlinearity in the medium, the stresses can not be calculated in a direct manner. The finite element method enables us to linearize the medium in a piecewise

manner and evaluate the effective non-linear characteristics. In view of the hysteresis curve of polarization of ferroelectric materials, three cases were investigated. These are (1) insulator subjected to a d.c. voltage (2) insulator subjected to an a-c voltage and the applied voltage goes from +ve maximum to -ve maximum and (3) when the applied voltage goes from the -ve maximum to +ve maximum. Peak value of the electromechanical stress takes place at the edge of parallel plate.

For the first two cases, the maximum stress occurs at the edge of the upper plate, but for the third case the maximum stress value occurs at the lower plate. It is also observed that the peak value of both electrical and mechanical stress rises if an alternating potential is applied. But the most severe case is when the applied potential goes from -ve maximum to +ve maximum. Here electromechanical stresses exceed the former two cases. These are illustrated in Figs. 4.4-4.9. For an alternating field, the electromechanical stresses converge to a constant value as the distance from the edge of parallel plates increases. This constant value of stress is due to the remanant polarization with the withdrawal of external field. Again from tables 4.2 and 4.3 of electromechanical stress angles, it is observed that during the time when the applied potential goes from +ve maximum to -ve maximum, the material between

the two parallel plates is subjected to compressive stress and when the applied potential goes from -ve maximum to +ve maximum, the material is subjected to a tensile stress. However, lateral stress in the radially outward direction is present in all the cases. Thus as the applied potential fluctuates, the dielectric material is subjected to repeated compression and expansion in the axial direction with a constant expanding tendency in the radial direction.

The finite element method is very useful technique for solving such type of boundary value problem where exact analytical solution is formidable. Energy calculation in insulators having different shapes and to find the optimum shape of insulators in light of the electromechanical stress analysis discussed above is of considerable interest. Hence the analysis may be extended to computer aided design of insulators.

APPENDIX - A

A.1 Laplace's equation for a charge free region is given by

$$\nabla^2 \phi = 0 \quad \dots \quad (1)$$

In variational form, the above eqn. (1) reduces to

$$\iint \nabla^2 \phi \delta \phi \, ds = 0 \quad \dots \quad (2)$$

$$\text{or} \quad \iint \delta \phi \nabla^2 \phi \, ds = 0 \quad \dots \quad (3)$$

Now, let us consider the identity

$$\nabla \cdot (a \nabla b) = a \nabla^2 b + \nabla a \cdot \nabla b \quad \dots \quad (4)$$

Let us put,  $a = \delta \phi$  and  $b = \phi$  in (4)

So, we get

$$\delta \phi \nabla^2 \phi = \nabla \cdot (\delta \phi \nabla \phi) - \nabla \delta \phi \cdot \nabla \phi$$

$$\text{or} \quad \delta \phi \nabla^2 \phi = \nabla \cdot (\delta \phi \nabla \phi) - \frac{1}{2} \delta (\nabla \phi)^2 \quad \dots \quad (5)$$

Let us now take a surface  $S$  enclosed by the contour  $C$  and let  $\bar{n}$  be the normal to the surface shown in Fig. 1

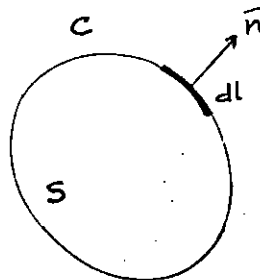


Fig. 1

Applying Gauss's Theorem over surface S

$$\int_S \nabla \cdot (\delta\phi \nabla\phi) ds = \int_C \vec{n} \cdot \nabla\phi \delta\phi dl \quad \dots \quad (6)$$

$$= \int_C \frac{\partial\phi}{\partial n} \delta\phi dl \quad \dots \quad (7)$$

Now applying relations (5) and (7), Laplace's equation in variational form (3) reduces to

$$\iint \left[ -\frac{1}{2} \delta(\nabla\phi)^2 \right] ds + \int_C \frac{\partial\phi}{\partial n} \delta\phi dl = 0 \quad \dots \quad (8)$$

$$\text{or } \delta \left\{ \frac{1}{2} \iint [(\nabla\phi)^2] ds \right\} - \int_C \frac{\partial\phi}{\partial n} \delta\phi dl = 0 \quad \dots \quad (9)$$

Let us now put the limiting conditions

(1)  $\phi = \text{constant}$  on the surface C giving

$$\delta\phi = 0 \quad (\text{Dirichlet})$$

(2)  $\frac{\partial\phi}{\partial n} = 0$  on surface C (Neumann)

Then eqn. (9) reduces to

$$\delta \left\{ \frac{1}{2} \iint [(\nabla\phi)^2] ds \right\} = 0 \quad \dots \quad (10)$$

Let us now suppose that the extremum functional be J such that  $\delta J = 0$ .

So, we get

$$J(\phi) = \frac{1}{2} \iint [(\nabla\phi)^2] ds \quad \dots \quad (11)$$

A.2 Determination of the tensor elements  $S_{ij}$  for ferroelectric insulators:

We have,

$$\begin{aligned} & D_z \left( \frac{\partial E_x}{\partial z} - \frac{\partial E_z}{\partial x} \right) - D_y \left( \frac{\partial E_y}{\partial x} - \frac{\partial E_x}{\partial y} \right) + E_x \nabla \cdot \bar{D} \\ &= D_z \frac{\partial E_x}{\partial z} - D_z \frac{\partial E_z}{\partial x} - D_y \frac{\partial E_y}{\partial x} + D_y \frac{\partial E_x}{\partial y} \\ &+ E_x \frac{\partial D_x}{\partial x} + E_x \frac{\partial D_y}{\partial y} + E_x \frac{\partial D_z}{\partial z} \quad \dots \quad (1) \end{aligned}$$

$$\begin{aligned} &= -D_z \frac{\partial E_z}{\partial x} - D_y \frac{\partial E_y}{\partial x} + E_x \frac{\partial D_x}{\partial x} + \frac{\partial}{\partial y} (E_x D_y) + \frac{\partial}{\partial z} (D_z E_x) \\ &\dots \quad (2) \end{aligned}$$

Now,

$$\begin{aligned} -D_z \frac{\partial E_z}{\partial x} &= -\epsilon_0 (\epsilon_{r0} E_z - k E_z^3) \frac{\partial E_z}{\partial x} \\ &= -\epsilon_0 \frac{\partial}{\partial x} \left( \frac{\epsilon_{r0}}{2} E_z^2 - \frac{k}{4} E_z^4 \right) \quad \dots \quad (3) \end{aligned}$$



Similarly

$$\begin{aligned}
 -D_Y \frac{\partial E_Y}{\partial x} &= -\epsilon_0 (\epsilon_{r0} E_Y - kE_Y^3) \frac{\partial E_Y}{\partial x} \\
 &= -\epsilon_0 \frac{\partial}{\partial x} \left( \frac{\epsilon_{r0}}{2} E_Y^2 - \frac{3}{4} k E_Y^4 \right) \dots \quad (4)
 \end{aligned}$$

$$E_X \frac{\partial D_X}{\partial x} = \epsilon_0 \frac{\partial}{\partial x} \left( \frac{\epsilon_{r0}}{2} E_X^2 - \frac{3}{4} k E_X^4 \right) \dots \quad (5)$$

Adding (3), (4) and (5) we get

$$\begin{aligned}
 &-D_Z \frac{\partial E_Z}{\partial x} - D_Y \frac{\partial E_Y}{\partial y} + E_X \frac{\partial D_X}{\partial x} \\
 &= \epsilon_0 \frac{\partial}{\partial x} \left[ -\frac{\epsilon_{r0}}{2} E_Z^2 + \frac{k}{4} E_Z^4 - \frac{\epsilon_{r0}}{2} E_Y^2 + \frac{k}{4} E_Y^4 \right. \\
 &\quad \left. + \frac{\epsilon_{r0}}{2} E_X^2 - \frac{3}{4} k E_X^4 \right] \\
 &= \epsilon_0 \frac{\partial}{\partial x} \left[ \epsilon_{r0} \left( E_X^2 - \frac{1}{2} E^2 \right) + \frac{k}{4} \left( E_Z^4 + E_Y^4 + E_X^4 - 3E_X^4 \right) \right] \dots \quad (6)
 \end{aligned}$$

where  $E = \sqrt{E_X^2 + E_Y^2 + E_Z^2}$

Thus

$$S_{11} = \epsilon_0 \left[ \epsilon_{r0} \left( E_X^2 - \frac{1}{2} E^2 \right) + \frac{k}{4} \left( E_Y^4 + E_Z^4 - 3E_X^4 \right) \right]$$

$$S_{12} = E_x D_y = \epsilon_0 (\epsilon_{ro} E_y - k E_y^3) E_x \quad \dots \quad (8)$$

$$S_{13} = D_z E_x = \epsilon_0 (\epsilon_{ro} E_z - k E_z^3) E_x \quad \dots \quad (9)$$

Similarly,

$$S_{21} = D_x E_y = \epsilon_0 (\epsilon_{ro} E_x - k E_x^3) E_y \quad \dots \quad (10)$$

$$S_{22} = \epsilon_0 \left[ \frac{\epsilon_{ro}}{2} (E_y^2 - \frac{1}{2} E^2) + \frac{k}{4} (E_z^4 + E_x^4 - 3E_y^4) \right] \quad \dots (11)$$

$$S_{23} = D_z E_y = \epsilon_0 (\epsilon_{ro} E_z - k E_z^3) E_y \quad \dots (12)$$

$$S_{31} = D_x E_z = \epsilon_0 (\epsilon_{ro} E_x - k E_x^3) E_z \quad \dots (13)$$

$$S_{32} = D_y E_z = \epsilon_0 (\epsilon_{ro} E_y - k E_y^3) E_z \quad \dots (14)$$

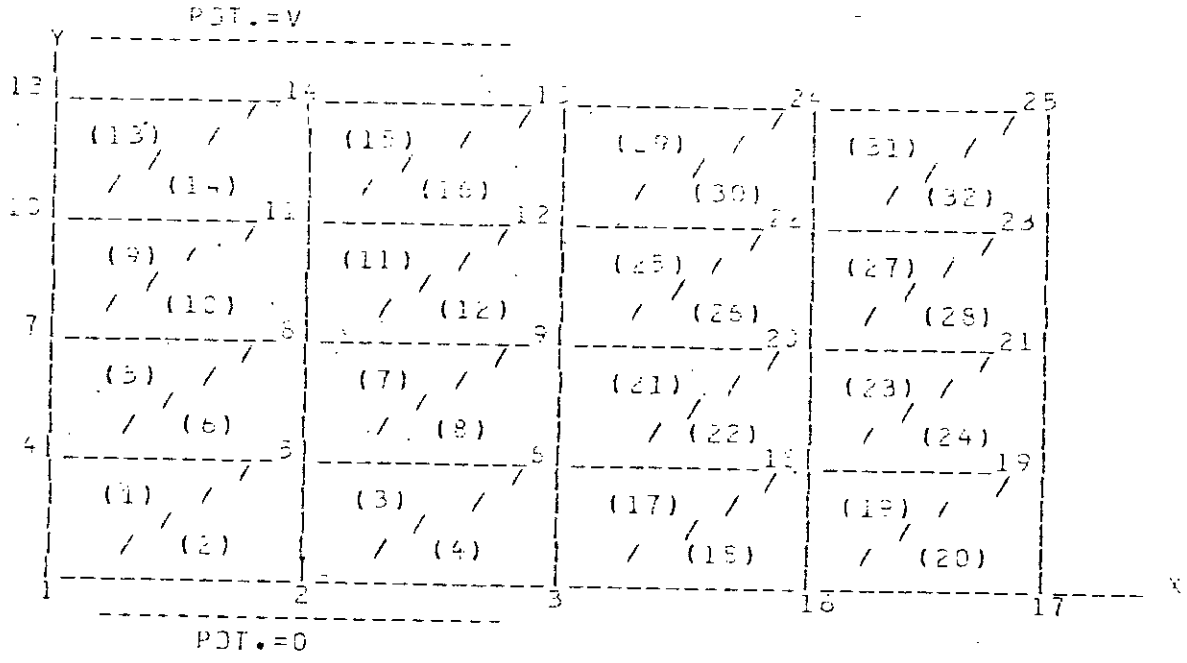
$$S_{33} = \epsilon_0 \left[ \epsilon_{ro} (E_z^2 - \frac{1}{2} E^2) + \frac{k}{4} (E_x^4 + E_y^4 - 3E_z^4) \right] \quad \dots (15)$$

FILE: #16 PLATHAN A1 BUET COMPUTER CENTER, CHENNAI

POT.=V

POT.=0

TWO PARALLEL PLATES



DIVISION INTO TRIANGULAR ELEMENTS  
 ( ) INDICATES ELEMENTS  
 NUMBERS INDICATE NODES

MAIN PROGRAM

```

DIMENSION V(45,45),C(45,45),XI(64),XJ(64),XK(64),YI(64),YJ(64),YK
+(64),I(64),J(64),K(64),ZA(45,90),ZI(45,45),VO(45),XA(45),HXI(64),
+HYI(64)
VO(1)=0.0
VO(2)=0.0

```

FILE: 805  
CONTINUE  
VD(13)=1100.0  
VD(14)=1100.0  
VD(15)=0.0  
DO E NV=4.12  
VD(V)=0.0  
CONTINUE  
VD(1)=19.45  
VD(2)=0.0  
CONTINUE  
71  
CONTINUE  
FILE: 803  
FORTRAN 41 SUEI COMPUTER CENTRE - DHAKA  
95























27 0.539E+04  
28 0.544E+04

FILE: BEG            DUT            A1 BUET COMPUTER CENTRE, DHAKA            VM/SP

29 0.545E+04  
30 0.544E+04  
31 0.541E+04  
32 0.546E+04  
33 0.547E+04  
34 0.550E+04  
35 0.550E+04  
36 0.550E+04  
37 0.550E+04  
38 0.566E+04  
39 0.558E+04  
40 0.554E+04  
41 0.553E+04  
42 0.573E+04  
43 0.561E+04  
44 0.556E+04  
45 0.555E+04

NON-LINEAR ELECTRIC FIELDS (V/M)

ELEMENTS	FIELD X	FIELD Y
1	-.203E+05	-.297E+06
2	0.200E+01	-.317E+05
3	-.102E+05	-.317E+05
4	-.322E+05	-.971E+05
5	0.317E+01	-.256E+06
6	-.203E+05	-.236E+06
7	0.513E+01	-.236E+06
8	-.102E+05	-.134E+05

FILE: BEG            DUT            A1 BUET COMPUTER CENTRE, DHAKA            VM/SP

0.203E+05            256E+01

11	0.102E+05	-.238E+05
12	0.513E+01	-.134E+05
13	0.200E+01	-.297E+05
14	0.203E+05	-.317E+05
15	0.322E+05	-.317E+05
16	0.102E+05	-.971E+05
17	-.658E+05	-.971E+05
18	-.127E+05	-.358E+05
19	-.344E+05	-.358E+05
20	-.552E+05	-.150E+05
21	0.513E+01	-.134E+05
22	-.658E+05	-.671E+05
23	0.473E+01	-.671E+05
24	-.344E+05	-.326E+05
25	0.658E+05	-.134E+05
26	0.513E+01	-.671E+05
27	0.344E+05	-.671E+05
28	0.473E+01	-.326E+05
29	0.127E+05	-.971E+05
30	0.658E+05	-.358E+05
31	0.552E+05	-.358E+05
32	0.344E+05	-.150E+05
33	-.159E+05	-.150E+05
34	-.251E+05	-.681E+04
35	-.795E+04	-.681E+04
36	-.115E+05	-.327E+04

FILE: B=6

OUT

.A1 BUET COMPUTER CENTRE, DHAKA

VM/SP (

37	-.347E+04	-.327E+04
38	-.496E+04	-.179E+04
39	-.972E+03	-.179E+04
40	-.138E+04	-.138E+04
41	0.434E+01	-.326E+05
42	-.159E+05	-.157E+05
43	0.355E+01	-.157E+05
44	-.795E+04	-.775E+04
45	0.239E+01	-.775E+04
46	-.347E+04	-.429E+04



48 0.972E+03 - .332E+04  
 49 0.159E+05 - .326E+05  
 50 0.434E+01 - .157E+05  
 51 0.795E+04 - .157E+05  
 52 0.355E+01 - .776E+04  
 53 0.347E+04 - .776E+04  
 54 0.239E+01 - .429E+04  
 55 0.972E+03 - .429E+04  
 56 0.200E+01 - .332E+04  
 57 0.251E+05 - .150E+05  
 58 0.159E+05 - .561E+04  
 59 0.115E+05 - .561E+04  
 60 0.795E+04 - .327E+04  
 61 0.496E+04 - .327E+04  
 62 0.247E+04 - .179E+04  
 63 0.138E+04 - .179E+04

FILE: BE5 DUT AI BUET COMPUTER CENTRE, DHAKA

VM/SP

64 0.972E+03 - .138E+04

MECHANICAL STRESS IN FERRO-ELECTRIC INSULATOR

ELEMENT	TT1	TT2	TT3	ANG
1	0.791E+03	0.234E+04	0.599E+04	82.09
2	0.347E+03	0.243E+04	0.591E+04	-90.04
3	0.937E+03	0.157E+04	0.684E+04	53.75
4	0.939E+03	0.159E+04	0.813E+04	-56.07
5	0.563E+03	0.266E+04	0.562E+04	-90.04
6	0.434E+03	0.258E+04	0.569E+04	60.11
7	0.460E+03	0.275E+04	0.552E+04	-90.04
8	0.248E+03	0.248E+04	0.535E+04	15.09
9	0.367E+03	0.283E+04	0.546E+04	-90.88
10	0.430E+03	0.275E+04	0.552E+04	-90.04
11	0.571E+03	0.356E+04	0.476E+04	-42.87

13	0.747E+03	0.290E+04	0.582E+04	-90.04
14	0.351E+03	0.280E+04	0.575E+04	-80.31
15	0.175E+04	0.157E+04	0.417E+04	1.14
16	0.175E+03	0.440E+04	0.871E+04	2.11

FILE: 000                    COT                    AI                    IJET COMPUTER CENTRE, DHAKA                    VM/SP

17	0.121E+03	0.298E+04	0.517E+04	21.70
18	0.155E+03	0.289E+04	0.549E+04	-58.59
19	0.218E+02	0.356E+04	0.459E+04	2.12
20	0.290E+02	0.352E+04	0.458E+04	-59.37
21	0.155E+03	0.326E+04	0.491E+04	-90.04
22	0.751E+02	0.312E+04	0.508E+04	1.12
23	0.398E+02	0.355E+04	0.449E+04	-90.04
24	0.199E+02	0.357E+04	0.457E+04	-3.15
25	0.195E+03	0.384E+04	0.435E+04	-37.40
26	0.398E+02	0.365E+04	0.449E+04	-90.04
27	0.503E+02	0.395E+04	0.421E+04	-35.55
28	0.941E+01	0.386E+04	0.427E+04	-90.03
29	0.227E+03	0.466E+04	0.374E+04	15.43
30	0.496E+02	0.443E+04	0.377E+04	32.92
31	0.393E+02	0.433E+04	0.355E+04	24.13
32	0.125E+02	0.427E+04	0.383E+04	42.84
33	0.452E+01	0.385E+04	0.430E+04	-5.60
34	0.599E+01	0.381E+04	0.432E+04	-59.69

35	0.9721+00	0.395E+04	0.417E+04	-8.94
36	0.127E+01	0.395E+04	0.418E+04	-58.25
37	0.202L+00	0.401E+04	0.411E+04	-3.40
38	0.245E+00	0.401E+04	0.412E+04	-50.32
39	0.367E+01	0.404E+04	0.408E+04	32.99
40	0.358E+01	0.404E+04	0.408E+04	-0.02
41	0.941E+01	0.386E+04	0.427E+04	-90.03
42	0.471E+01	0.382E+04	0.431E+04	-4.05
43	0.219E+01	0.396E+04	0.416E+04	-90.02
44	0.109E+01	0.395E+04	0.418E+04	-1.45
45	0.534E+00	0.401E+04	0.411E+04	-90.01
46	0.270E+00	0.401E+04	0.412E+04	12.03
47	0.153E+00	0.404E+04	0.409E+04	-89.99
48	0.108E+00	0.403E+04	0.409E+04	57.35
49	0.119E+02	0.400E+04	0.418E+04	-35.26
50	0.219E+01	0.396E+04	0.416E+04	-90.01
51	0.275E+01	0.403E+04	0.410E+04	-35.29
52	0.734E+00	0.401E+04	0.411E+04	-89.99
53	0.541E+00	0.404E+04	0.405E+04	-41.80

54	0.153E+00	0.404E+04	0.409E+04	-89.98
55	0.171E+00	0.404E+04	0.406E+04	-64.50
56	0.977E-01	0.404E+04	0.408E+04	-89.98
57	0.759E+01	0.418E+04	0.395E+04	28.18

50	0.155E+01	0.412E+04	0.401E+04	28.76
60	0.557E+00	0.411E+04	0.401E+04	45.84
51	0.512E+00	0.400E+04	0.404E+04	23.74
62	0.135E+00	0.400E+04	0.404E+04	35.10
63	0.453E-01	0.406E+04	0.406E+04	-14.70
64	0.255E-01	0.406E+04	0.406E+04	-19.72

ELEMENTS	ENERGY
1	8752470.0000
2	9952712.0000
3	10955107.0000
4	11204020.0000
5	5485957.0000
6	5533426.0000
7	5492131.0000
8	2794464.0000
9	6527479.0000

FILE: BEG                    DUT                    A1    BUET COMPUTER CENTRE, DHAKA                    VM/SP (4

10	5492321.0000
11	6524856.0000
12	1762121.0000
13	8721893.0000
14	10004945.0000
15	23231248.0000
16	1970293.0000
17	1369269.0000
18	1734520.0000
19	245540.4370
20	327132.3750
21	1762069.0000
22	981093.8750
23	449475.9370
24	22+888.1870
25	2193831.0000
26	449475.9370

REFERENCES

- [1] M. Ieda and M. Nawata, "DC Treeing Breakdown Associated with Space Charge Formation in Polyethylene" IEEE Trans. Ins. Vol. EI-12, PP. 19-25, 1977.
- [2] M. Ieda, "Dielectric Breakdown Process of Polymer" IEEE Trans. Elec. Ins. Vol. EI-15, PP. 206-224, 1980.
- [3] H. Singer, H. Steinbigler and P. Weiss, "A Charge Simulation Technique for Calculation of High Voltage Fields", IEEE Trans., Vol. PAS-93, PP. 1660-1668, 1974.
- [4] M. Abdel-Salam and E.K. Stanek, "Optimizing Field Stress on High Voltage Insulators", IEEE Trans., Vol. EI-22, No. 1, PP. 47-56, 1987.
- [5] P.K. Mukherjee and C.K. Roy, "Computation of Fields in and around Insulators by Fictitious Point Charge Method", IEEE Trans., Vol. EI-13, No.1, 1978.
- [6] Takeshi Takashima and Ryoza Ishibashi, "Electric Fields in Dielectric Multilayers Calculated by Digital Computers", IEEE Trans, Vol. EI-13, No.1,1978.
- [7] Tadsu Takuma, "Field behaviour near Singular Points in Composite Dielectric Arrangements", IEEE Trans., Vol. EI-13, No.6, 1978.
- [8] Heng-Kun Xie, Xin-Shan Ma and Kwan C.Kao, "Computation of Electric Fields and Study of Optimal Corona Suppression for Bushing Type Insulators", IEEE Trans., Vol. EI-21, No.1, PP. 41-51, 1986.

- [9.] D.D. Chang, T.S. Sudarshan and J.E Thompson,  
"Analysis of Electrical Stress Distribution in  
Cavities Embeded Within Dielectric Structures",  
IEEE Trans., Vol. EI-21, No.2, 1986.
- [10.] S. Ahmed and P. Daly, "Waveguide Solutions by Finite  
Element Method", The Radio and Electronic Engineering,  
Vol. 38, No. 4, 1969.
- [11.] M. Abdel-Salam, M. Farghally and S. Abdel-Sattar,  
"Finite Element Solution of Monopolar Corona Equation",  
IEEE Trans., Vol. EI-18, No.2, 1983.
- [12.] S. Ahmed, "Finite Element Method for Waveguide Problems",  
Electronics Letter, Vol. 4, No. 18, 1968.
- [13.] R.H. Gollagher, "Finite Element Analysis", Prentice-  
Hall, Englewood Clifi, New Jersey, 1975.
- [14.] D.H. Norrie and G.De Vries, "An Introduction to Finite  
Element Analysis", Academic Press, 1978.
- [15.] K.W. Wargner, "The Physical Nature of Electrical  
Breakdown of Solid Dielectrics", AIEE Trans., Vol.41,  
PP. 288-299, 1922.
- [16.] K.H. Stark and C.G. Garton, "Electric Strength of  
Irradiated Polythene", Nature, Vol. 176, PP. 1225-1226,  
1955.
- [17.] Allan Greenwood, "A Perspective on Insulation Systems  
in the Electric Power Industry", IEEE Trans, Vol. EI-15  
No.3, 1980.
- [18.] Adrianus J. Dekker, "Electrical Engineering Materials",  
Prentice-Hall of India, New Delhi-110001, 1977.

- [19]. Simon Ramo, John R. Whinnery, Theodore Van Dyzer, "Fields and Waves in Communication Electronics", John Wiley and Sons, Inc. New York, 1965.
- [20]. S.Ahmed and P. Daly, "Finite Element Method for Inhomogeneous Waveguides", Proc. IEE, Vol. 116, No.10, 1969.
- [21]. N. Mabaya, P.E. Lagasse , and P. Vandembuleke, "Finite Element Analysis of Optical Waveguides", IEEE Trans. on Microwave Theory and Techniques, Vol. MTT-29, No.6, 1981.
- [22]. J.A. Stratton, "Electromagnetic Theory", McGraw-Hill Book Co. New York and London, 1941.
- [23]. R.E. Collin, "Field Theory of Guided Waves", McGraw-Hill Book Co., New York, 1960.
- [24]. L.J. Segerlind, "Applied Finite Element Analysis" John Wiley & Sons, Inc. 1976.
- [25]. O. W. Anderson, "Finite Element Solution of Complex Potential Electric Fields", IEEE Trans., Vol. PAS-96, PP 1156-1161, 1977.

